Critical Reviews in Environmental Science and Technology, 25(2):141–199 (1995)

A Review: Pyrite Oxidation Mechanisms and Acid Mine Drainage Prevention

V. P. (Bill) Evangelou and Y. L. Zhang*
Department of Agronomy, University of Kentucky, Lexington

* Address correspondence to: V. P. Evangelou, Department of Agronomy, N-122 Ag. Sci. Center North, University of Kentucky, Lexington, KY 40546-0091.

ABSTRACT: Sulfide oxidation, part of sulfur's biotic/abiotic cycle, is an important natural phenomenon. However, because of the sulfide's association with metallic ores and fossil fuels in the form of pyrite (FeS_2) and the world's increasing demand for metals and fossil fuels, sulfide oxidation in nature is in some state of perturbation. This perturbation, which results from land disturbances (e.g., mining, and/or ore processing), produces acid drainage often enriched with heavy metals. This acid drainage, commonly referred to as acid mine drainage (AMD), has become an economic and environmental burden. This review deals with abiotic/biotic modes of pyrite oxidation and the mechanistic involvement of OH^-, O_2, and Fe^{3+} in the pyrite oxidation process in low/high pH environments. Also included is recent evidence on the potential involvement of CO_2 in catalyzing pyrite oxidation in near-neutral and alkaline environments. Finally, the review deals with various pyrite-oxidation control approaches, the merits of these approaches, and some new and promising pyrite microencapsulation techniques currently under development in our laboratory.

KEY WORDS: pyrite surface chemistry, coating technologies, pyrite morphology, bacterial and abiotic oxidation of pyrite, prevention technologies of acid mine drainage.

I. INTRODUCTION

Pyrite oxidation and the factors affecting its rate have been studied extensively because of their importance in environmental quality and mineral recovery. Pyrite, iron disulfide (FeS_2), is commonly associated with coal and metal ore deposits, and its oxidation results in acid drainage formation, a significant environmental pollution problem. Such extremely acidic drainage (as low as pH 2) is often enriched with Fe, Mn, Al, SO_4, and sometimes heavy metals such as Pb, Hg, Cd, etc. Discharge of acid drainage into streams, rivers, and lakes causes an instant threat to the biota and ecological balance.

Throughout the world, large sums of money are spent yearly for preventing acid drainage formation at its source or treating acid drainage already formed. Conversely, microbiological and chemical oxidation of pyrite and other metal disulfides or metal sulfides is beneficial in depyritizing/desulfurizing coal and in the commercial recovery of metals from low-grade ores and wastes. Pyrite oxidation is also important in geochemistry, marine chemistry, and soil science with

1064-3389/95/$.50

respect to natural mineral weathering, sulfur cycling and sulfur detoxification, and soil development/quality, respectively. Environmental awareness and industrial application of pyrite oxidation technologies have stimulated research in the control mechanisms of pyrite oxidation. This review focuses on mechanisms of pyrite oxidation and current practices for preventing acid drainage formation.

Pyrite oxidation takes place when the mineral is exposed to air and water. The process is complex because it involves chemical, biological, and electrochemical reactions, and varies with environmental conditions. Factors such as pH, $^{P}O_2$, specific surface and morphology of pyrite, presence or absence of bacteria and clay minerals, as well as hydrological factors determine the rate of oxidation. There is, therefore, no single rate law available to describe the overall kinetics of pyrite oxidation for all cases.

The chemical reactions governing pyrite oxidation are (Reference 129 and references therein):

$$FeS_2 + 7/2O_2 + H_2O \rightarrow Fe^{2+} + 2SO_4^{2-} + 2H^+ \tag{1}$$

$$Fe^{2+} + 1/4O_2 + H^+ \rightarrow Fe^{3+} + 1/2H_2O \tag{2}$$

$$Fe^{3+} + 3H_2O \rightarrow Fe(OH)_3(s) + 3H^+ \tag{3}$$

$$\begin{aligned} &FeS_2 + 7Fe_2(SO_4)_3 \\ &\quad + 8H_2O \rightarrow 15FeSO_4 + 8H_2SO_4 \end{aligned} \tag{4}$$

Although the above four reactions are mass and charge balanced, they do not have any molecular mechanistic meaning, nor do they have any rate reaction meaning. Reactions 1 and 4 indicate that Fe^{3+} and O_2 are the major oxidants of pyrite. Reaction 1 shows the direct reaction of O_2 with pyrite to produce Fe^{2+}, which is then oxidized to Fe(III) by O_2, as shown in Reaction 2. Finally, Reaction 3 shows $Fe(OH)_3$ precipitate formation.

At low pH (<4.5), Fe^{3+} oxidizes pyrite much more rapidly than O_2 and more rapidly than O_2 oxidizes dissolved Fe^{2+} to Fe^{3+} (Figure 1).[113] For this reason, Reaction 2 is known to be the rate-limiting step in abiotic pyrite oxidation.[129] However, iron-oxidizing bacteria, especially *Thiobacillus ferrooxidans*, can accelerate the rate of Fe^{2+} oxidation by a factor of 10^6.[35,129] *T. ferrooxidans* is an acidophilic chemolithotrophic organism that is ubiquitous in geologic environments containing pyrite.[113] Thus, in the presence of *T. ferrooxidans* and under low pH conditions, pyrite oxidation can be described by Reactions 2 and 4.

At neutral to alkaline pH, the abiotic rate of Fe^{2+} oxidation rises rapidly (Figure 1), but Fe^{3+} concentration also decreases greatly due to the precipitation of ferric hydroxide as described by Reaction 3. Because there is probably very little bacterial participation in pyrite oxidation at neutral to alkaline pH, some research-

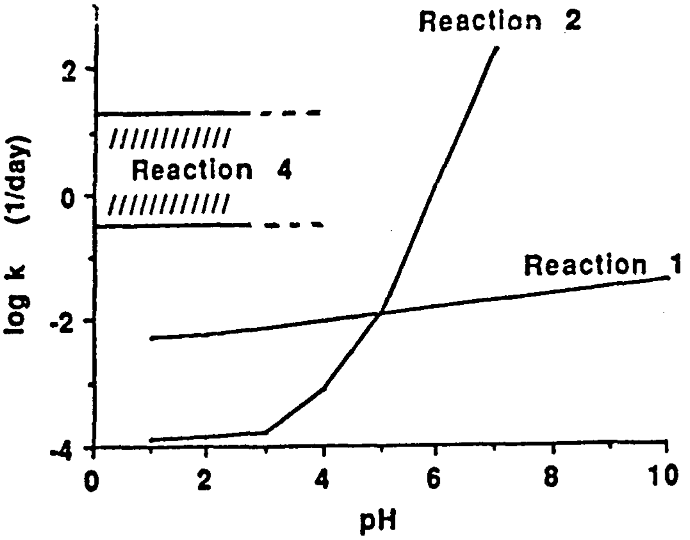

FIGURE 1. Comparison of rate constants as a function of pH for reaction 4, oxidation of pyrite by Fe^{3+}; reaction 2, oxidation of Fe^{2+} by O_2; and reaction 1, oxidation of pyrite by O_2. Reactions 1, 2, and 4 are given in the text. (From Nordstrom, D. K., in *Acid Sulfate Weathering: Pedogeochemistry and Relationship to Manipulation of Soil Minerals,* Hossner, R. L., Kittrick, J. A., and Fanning, R. F., Eds., Soil Science Society of America Press, Madison, WI, 1982, 46. With permission.)

ers suggested that in such environments O_2 is a more important pyrite oxidant than Fe^{3+}.[57,70] This suggestion, however, is contradicted by recent findings that pointed out that Fe^{3+} is the preferred pyrite oxidant at circumneutral pH, and the major role played by O_2 is to oxidize Fe^{2+} and thereby sustain the pyrite oxidation cycle.[95,96,105,106]

Finally, Reaction 3, taking place at pH values as low as 3, is a readily reversible dissolution/precipitation reaction that serves as a source as well as a sink of solution Fe^{3+}, and is a major step in the release of acid to the environment.

II. OCCURRENCE, FORMATION, AND MORPHOLOGY OF PYRITE

The two major forms of iron disulfide (FeS_2) in geologic strata are pyrite and marcasite. Both minerals have the same chemical composition, but differ crystallographically. The structure of marcasite is orthorhombic, while that of pyrite is isometric.[141] Because of its particular structure, marcasite is less stable than pyrite. Based on crystallographic examinations, pyrite is the most prevalent form present in coals.[61,62,90]

Pyrite is generally associated with coal fields in the U.S. and elsewhere in the world. Pyrite is also associated with many ores including zinc, copper, uranium, gold, and silver. In the eastern coal fields of the U.S., pyrite is most commonly found associated with the geologic strata adjacent to, immediately above, or below the coal seam (see Reference 47 and references therein). A pyrite-rich layer in Pennsylvania-age shales in Missouri was found capped with limestone.[1] Caruccio and Geidel[24,25] reported that pyrite is not uniformly distributed throughout a geologic stratum as one observes with blanket deposits of calcium carbonate, but rather in clusters or scattered pockets of accumulation. A horizontal variation of pyritic content of up to 4% has been found within centimeters from one sampling to another, whereas the vertical variation of pyritic content of geologic strata appears to be of a lesser magnitude.

Pyrite is formed in a reducing environment with a continuous supply of sulfates and iron in the presence of easily decomposable organic matter. Barriga and Fyfe[9] proposed that iron sulfide precipitation may have taken place under a thin veneer of siliceous sediments. The carbon-to-sulfur ratio, availability of iron, and oxidation potential are the major factors that determine the rate of pyrite formation. For typical anoxic marine sediments overlain by oxic water, the major processes involved in the formation of sedimentary iron sulfide were summarized by Berner[12] in the following three steps: (1) reduction of sulfate to sulfide by bacteria, (2) reaction of the hydrogen sulfide with iron minerals to form iron monosulfides, and (3) reaction of the iron monosulfides with elemental sulfur to form pyrite.

It is generally accepted that a limited supply of organic carbon in marine sediments results in a lower rate of sulfate reduction. Pyrite formation in such environments is considered a slow process, giving rise to framboidal pyrite (strawberry-like).[13,55,58] On the other hand, in salt marshes where organic matter content is high and sulfate reduction is rapid, pyrite is believed to form rapidly, hours to days, via precipitation of iron with polysulfides. This direct precipitation normally gives rise to small single pyrite crystals.[55,71,122] The difference in the mechanisms of pyrite formation between marine and marsh sediments can be partially explained by the low pH of marsh sediments that keep the solution undersaturated with respect to monosulfides but supersaturated with respect to pyrite.[71,94] Finally, the rate of pyrite formation in freshwater sediments is much lower than that in marine sediments due to the fact that in fresh water, sulfate concentrations are two to three orders of magnitude lower than in seawater.

Pyrite can vary significantly in grain size and morphology, depending on the environment of formation. Arora et al.[2] reported that pyrite occurred as acicular forms, coarse-grained masses, euhedral forms, framboids and polyframboids, and octahedral and pyritohedral crystals (Figure 2). They also reported that pyrite isolated from lignite coal was composed of porous and nonporous irregular grains. Ainsworth and Blanchar[1]studied the morphology of pyrite isolated from Pennsylvanian-age shale in Missouri and reported their findings in terms of three pyrite groups: (1) pyrite with a smooth crystal surface, which includes octahedral, cubic and pyritohedral, (2) conglomerates with irregular surfaces composed of many

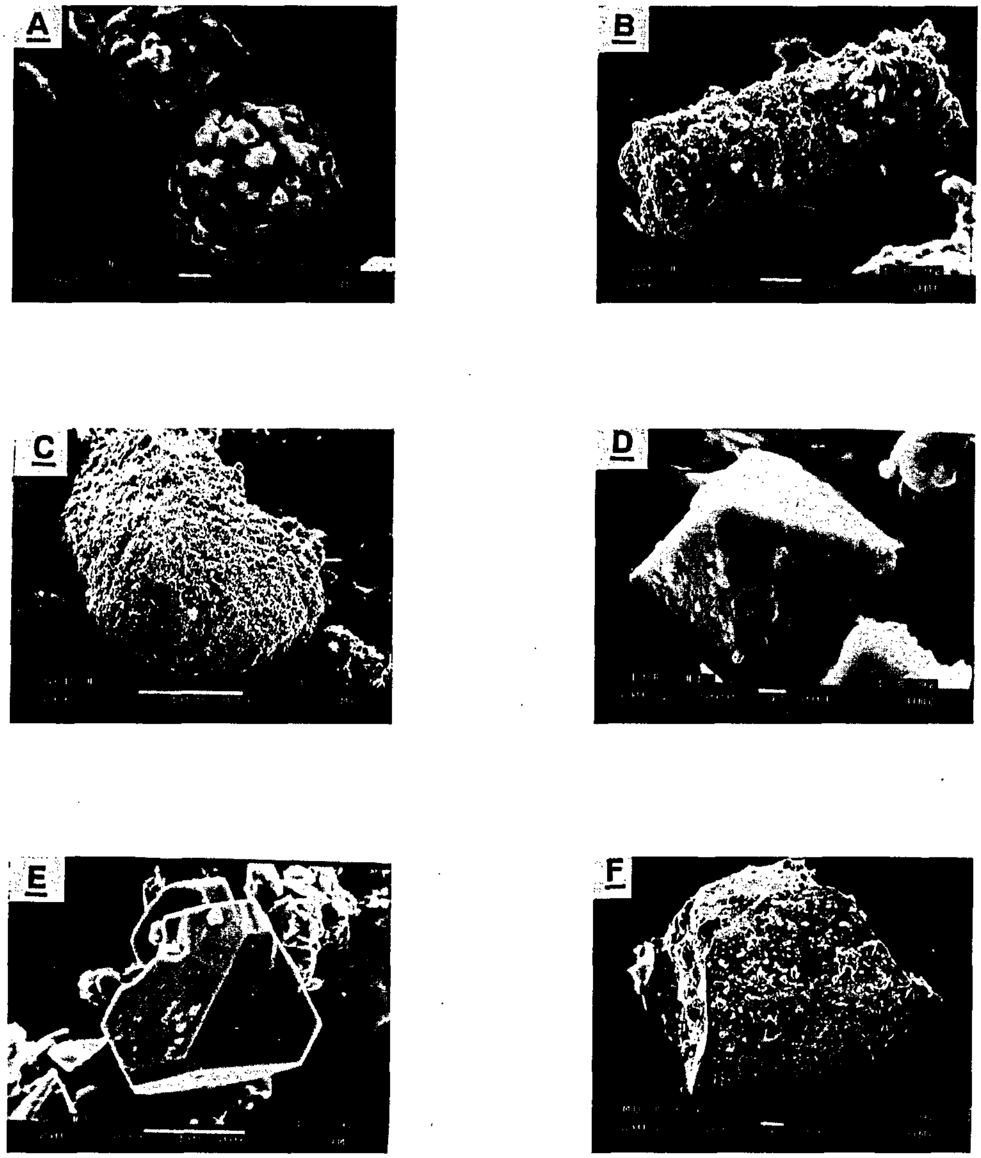

FIGURE 2. Various forms of pyrite. (A) Framboid with high surface area and high porosity; (B) polyframboid, a cluster of framboids; (C) conglomerate with irregular surface; (D, E) octahedron and pyritohedron with smooth surface; (F) massive Missouri museum pyrite with little or no surface porosity. (From Zhang, Y. L., Blanchar, R. W., and Hammer, R. D., in Proceedings of the 10th National Meeting of the American Society of Surface Mining and Reclamation, Vol. 2, Spokane, WA, May 16 to 19, 1993, 284.)

cemented particles, and (3) framboids in which the cemented crystals formed a smooth sphere. They also reported that the conglomerates were the predominant form. Zhang et al.[159] characterized the chemical and morphological properties of pyrite separated from scrubber sludge, gob, and slurry of coal residue. Their results indicated that scrubber sludge contained a trace amount of pyrite in the form of smooth-rounded, conglomerates, and framboidal forms. Both gob and slurry contained 2 to 5% pyrite, with the predominant forms of conglomerates and framboids or polyframboids. Numerous octahedral, cubic, pyritohedral, and twinned crystals were also found. Chemical and physical analyses of the above pyrite samples by Zhang et al.[159] also indicated that these pyrite coal residues had crystal structures, forms, and compositions similar to those commonly described for pyrite.

Framboid and polyframboid pyrites are of interest because they are more reactive than conglomeritic pyrite due to a high specific surface and high porosity.[27] It has been well documented that pyrite oxidation is a surface-controlled reaction.[69,105,106,129]

III. MECHANISMS OF PYRITE OXIDATION

A. Mechanisms of Bacterial Pyrite Oxidation

Mechanisms of bacterial pyrite oxidation have mainly been derived from investigations of metal bioleaching. The most widely studied pyrite-oxidizing bacterium is *T. ferrooxidans*. *T. ferrooxidans* is an obligate chemoautotrophic and acidophilic, and it is now well established that it is able to oxidize Fe^{2+}, S^o, and metal sulfides as well as other reduced inorganic sulfur compounds. *T. Thiooxidans* has also been isolated from acid mine wastes and has been studied extensively with respect to its pyrite oxidation potential. It has been determined that *T. Thiooxidans* can oxidize both elemental sulfur and sulfide to sulfuric acid ($S^o + 1.5O_2 + H_2O \rightarrow H_2SO_4$ and $S^{2-} + 2O_2 + 2H^+ \rightarrow H_2SO_4$).[15,92] Unlike *T. ferrooxidans*, *T. thiooxidans* cannot oxidize Fe^{2+}.[66]

The mechanisms of bacterial pyrite oxidation have been studied extensively,[31,59,82,108,151–153] and the results have been discussed and summarized in a number of articles.[39,93,113] Generally, the mechanisms of pyrite oxidation by bacteria are classified into direct metabolic reactions and indirect metabolic reactions. Direct metabolic reactions require physical contact between bacteria and pyrite particles, while indirect metabolic reactions do not. With indirect metabolic reactions, bacteria oxidize Fe(II) to Fe(III), thereby regenerating the Fe^{3+} required for the chemical oxidation of pyrite.[129] More details on direct and indirect metabolic pyrite oxidation are given in the reactions below without considering complete mass or charge balance.

1. Direct Metabolic Oxidation

According to Torma[148] and references therein, direct metabolic pyrite oxidation can be given by:

$$FeS_2 + O_2 \xrightarrow{\text{Bacteria}} Fe^{2+} + 2SO_4^{2-} + H^+ \qquad (5)$$

Reaction 5 consists of the dissolution of iron disulfide (FeS_2), as shown in Reaction 6 below,

$$FeS_2 \rightarrow Fe^{2+} + S_2^{2-} \qquad (6)$$

and the released disulfide anion shown in Reaction 6 is immediately bound by bacterial enzymes and oxidized to sulfate, as shown in Reaction 7.[127,148]

$$S_2^{2-} + 4O_2 \xrightarrow{\text{Bacteria}} 2SO_4^{2-} \qquad (7)$$

Theoretically, the process described by Reactions 6 and 7 can be continued until all disulfide is converted to sulfate. Konishi et al.[82] suggested that direct microbial pyritic sulfur oxidation to sulfate was due to the multiplication of *T. ferrooxidans* on the pyrite surface using pyritic sulfur as nutrient. Konishi et al.[82] however, did not mention if dissolution of the disulfide mineral occurred prior to microbial oxidation of the disulfide anion. Palencia et al.[116] suggested that pyrite is directly attacked by oxidizing bacteria, according to Reaction 8 shown below

$$4FeS_2 + 15O_2 + 2H_2O \rightarrow 2Fe_2(SO_4)_3 + 2H_2SO_4 \qquad (8)$$

Reaction 8 is the sum of the bacteria-catalyzed oxidation of sulfur and iron by O_2. It is believed that this direct pyrite oxidation mechanism contributes more to pyrite oxidation due to its involvement of iron oxidation.

Attachment of *T. ferrooxidans* on the pyrite surface and consequent oxidative corrosion have been investigated by many workers.[11,31,82,108,151,152] Bennett and Tributsch[11] confirmed that the chemical processes taking place on the pyrite surface due to oxidizing bacteria occur mainly in the region of contact between bacteria and pyrite. The same authors also suggested that the bacterial distribution on the pyrite surface is critically dependent on the crystal structure and the diversity in the crystal orders (fracture lines, dislocations) of the pyrite. Konishi et al.[82] indicated that *T. ferrooxidans* may multiply on the pyrite surface as well as in the liquid phase. Their data on dissolution kinetics of pyrite by *T. ferrooxidans* in a batch reactor indicated that the concentration of bacteria in the liquid phase could be related to the concentration of bacteria adsorbed onto the pyrite surface. Observations by scanning electron microscopy of pyrite particles inoculated with *T. ferrooxidans* revealed the appearance of corrosion, cracks, and small pits on the pyrite surfaces. Mustin et al.[108] indicated that the specific surface areas of pyrite before and after bioleaching were 1.1 and 1.6 m²/g, respectively. Thus, bacterial oxidation increased the porosity and specific surface in pyrite grains.

2. Indirect Metabolic Oxidation

In the case of indirect metabolic oxidation (see Reference 148 and references therein), pyrite is chemically oxidized by Fe^{3+} according to Reactions 9 and 10 shown below

$$FeS_2 + Fe_2(SO_4)_3 \rightarrow 3FeSO_4 + 2S^o \tag{9}$$

and

$$2S^o + 6Fe_2(SO_4)_3 8H_2O \rightarrow 12FeSO_4 + 8H_2SO_4 \tag{10}$$

Note that summing the above two reactions produces Reaction 4. The ferrous iron and elemental sulfur, S^o, produced by these chemical reactions are oxidized by *T. ferrooxidans*, thus regenerating Fe^{3+} and acid. These oxidation reactions may take place on the pyrite surface or in the interstitial solution and are as follows:

$$4FeSO_4 + 2O_2 + 2H_2SO_4 \rightarrow 2Fe_2(SO_4)_3 + 2H_2O \tag{11}$$

and

$$2S^o + 3O_2 + 8H_2O \rightarrow 2H_2SO_4 \tag{12}$$

The role of bacteria in oxidizing pyrite can, therefore, be seen as indirect; their function is to regenerate Fe^{3+}, the major pyrite oxidant. Reactions 4 or 9 have been found to occur in sterile tests, inoculated tests, and anaerobic tests. Note that reaction 4 is the common way to describe oxidation of pyrite by Fe^{3+}, through pyrite dissolution mainly by Reaction 9, S^o oxidation by Fe^{3+} through Reaction 10, reoxidation of Fe^{2+} by Reaction 11 and oxidation of part of sulfur by Reaction 12.[86,128]

The relative contributions by each of the mechanisms of direct and indirect metabolic pathways to pyrite oxidation remain disputed. Silverman[128] reported that the two mechanisms of pyrite oxidation may operate concurrently. On the other hand, Carranza[22] reported that the direct metabolic contact mechanism is the main operative mechanism for the oxidation of pyrite in the presence of *T. ferrooxidans*. Wakao et al.[151-153]indicated that the concentration of *T. ferrooxidans* in an aqueous phase, rather than on the surface of pyrite particles, plays a major role in enhancing pyrite oxidation through the indirect metabolic pathway. They based their conclusion on their observation that cells of *T. ferrooxidans* adsorbed onto the pyrite surface did not proliferate and their oxidizing activity was strongly inhibited.

B. Electrochemical Mechanism of Pyrite Oxidation

According to Lowson,[91] the overall electrochemical oxidation process of pyrite is the sum of the cathodic and anodic reactions occurring at the surface. The anodic process is a complex collection of oxidation reactions in which the pyrite reacts mainly with water to produce Fe^{3+}, sulfates, and protons, as shown by Equation 13,

$$FeS_2(s) + 8H_2O \rightarrow Fe^{3+} + 2SO_4^{2-} + 16H^+ + 15e^- \qquad (13)$$

or to produce Fe^{2+} and S^o when the acid strength increases,[6] as shown by Equation 14

$$FeS_2(s) \rightarrow Fe^{2+} + 2S^o + 2e^- \qquad (14)$$

The electrons are then transferred to a cathodic site (at the mineral surface or on the bacteria), where the principal reaction is an oxygen reduction process shown by Reaction 15

$$O_2(aq) + 4H^+ + 4e^- \rightarrow 2H_2O \qquad (15)$$

It should be noted that in electrochemical pyrite oxidation reactions, dissolved O_2 is only employed as an electron acceptor in a separate cathodic reaction, as shown by Reaction 15; the oxygen in the SO_4^{2-} is derived from water in an anodic reaction, as shown by Reaction 13.

C. Galvanic Effect on Metal-Disulfide Dissolution

Physical contact between two different metal-disulfide minerals in an acid/ferric sulfate solution creates a galvanic cell. This galvanic cell results in a selective electrochemical dissolution of the metal-disulfide minerals.[100,147] According to Torma[148] and Mehta and Murr,[100] in the case of two metal-disulfide minerals with different electrical rest potentials, the mineral with the lower electrical rest potential, acting as anode, will be dissolved, while the mineral with higher rest potential, acting as a cathode, will be galvanically protected. For example, Torma[148] pointed out that in the case of chalcopyrite/pyrite galvanic cell ($CuFeS_2/FeS_2$), chalcopyrite, with lower rest potential, will dissolve rapidly while pyrite will remain practically intact. Furthermore, Torma (1988) pointed out that the role of bacteria in the galvanic cell is to continuously oxidize the elemental sulfur (produced from the anodic oxidation reaction) to sulfate; thus, formation of a sulfur barrier on the surface of chalcopyrite is eliminated.

The galvanic reaction of the $CuFeS_2/FeS_2$ cell can be described by an anodic oxidation reaction on the $CuFeS_2$ surface and a cathodic oxygen reduction on the surface of FeS_2 (see Reference 148 and references therein). The anodic oxidation reaction on the chalcopyrite surface can be expressed by:

$$CuFeS_2 \rightarrow Cu^{2+} + Fe^{2+} + 2S^{\circ} + 4e^{-} \tag{16}$$

while the cathodic oxygen reduction taking place on the surface of pyrite is given by:

$$O_2 + 4H^{+} + 4e^{-} \rightarrow 2H_2O \tag{17}$$

Thus, the sum of the galvanic reaction can be expressed as:

$$CuFeS_2 + O_2 + 4H^{+} \rightarrow Cu^{2+} + Fe^{2+} + 2S^{\circ} + 2H_2O \tag{18}$$

The elemental sulfur (S^{o}) and ferrous iron shown in Reaction 18 will be oxidized by bacteria according to Reactions 11 and 12.

Pyrite is the most abundant disulfide mineral and is associated in varying amounts with other sulfide minerals, such as those of copper, nickel, and zinc, or with uranium ores. The quantitative contribution of galvanic reactions in the dissolution of metal disulfides or metal sulfides in these natural environments are unknown. It is most likely that in these systems different mechanisms of oxidative/dissolution operate simultaneously. These mechanisms may include galvanic dissolution, electrochemical oxidation, and oxidation by Fe^{3+}, O_2, and bacteria.

D. Kinetics of Fe^{2+} to Fe^{3+} Oxidation

1. Kinetics of Abiotic Oxidation of Fe^{2+} to Fe^{3+}

Understanding the kinetics of oxidation of Fe^{2+} to Fe^{3+} is important because, as pointed out previously, Fe^{3+} is the major pyrite oxidant. It is widely accepted that Fe^{3+} at low pH (<4.5) oxidizes pyrite much more rapidly than O_2.[129] However, recent findings also revealed that Fe^{3+} may be the preferred pyrite oxidant at circumneutral pH. In systems such as acid water, pyritic mine waste, and fresh water, abiotic and biotic oxidation of Fe^{2+} with O_2 may occur simultaneously with different kinetics, depending upon the environment. Pesic et al.,[117] after reviewing the literature, described the oxidation rate of Fe^{2+} with O_2 in the absence of bacteria with two major expressions. The first rate expression describing the oxidation of Fe^{2+} in an acidic medium, under atmospheric or elevated partial pressures of O_2 (${}^{P}O_2$), was given by:

$$-\left(d\left[Fe^{2+}\right]\right)/dt = k\left(\left[Fe^{2+2}\right]\right)/\left[H^{+}\right]^{1/4} {}^{P}O_2 \tag{19}$$

where k is the rate reaction constant. The second rate expression describing the oxidation of Fe^{2+} at neutral or higher than neutral pH was given by:

$$-\left(d\left[Fe^{2+}\right]\right)/dt = k\left[Fe^{2+}\right]\left[OH^{-}\right]^{2}\,{}^{P}O_{2} \qquad (20)$$

The above two rate expressions (Equations 19 and 20) show that under acid or neutral to alkaline conditions, the rates of Fe^{2+} oxidation are dependent on Fe^{2+} concentration, pH, and ${}^{P}O_2$. The hydrogen ion has a negative effect on the oxidation rate in acidic, neutral, or alkaline conditions. The major difference between Reactions 19 and 20 is that the reaction described by Equation 19 is second order with respect to Fe^{2+}, while the reaction described by Equation 20 is first-order with respect to Fe^{2+}.

2. Kinetics of Bacterially Mediated Oxidation of Fe^{2+}

Pesic et al.,[117] using an electrochemical method to measure the oxidation rate of Fe^{2+} to Fe^{3+} by O_2 in the presence of *T. ferrooxidans*, determined that the rate is directly proportional to the concentration of bacteria, Fe^{2+}, O_2, and H^+. They also reported that above pH 2.2, the oxidation of Fe^{2+} was governed by the following rate expression:

$$-d\left[Fe^{2+}\right]/dt = [1.62]\left[10^{11}\right]\left[C_{bact}\right]\left[H^{+}\right]\left[Fe^{2+}\right]\left[{}^{P}O_{2}\right]e^{-(58.77/RT)} \qquad (21)$$

where C_{bact} denotes bacteria concentration, T is absolute temperature, and R is the universal gas constant. Below pH 2.2, the rate expression is the same as the one above pH 2.2 except that it is independent of pH.

The halftime, the time required to achieve 50% conversion of initial reactant, can be used to demonstrate the importance of pH and *T. ferrooxidans* during the oxidation of Fe^{2+} with O_2. The halftime of 0.001 *M* Fe^{2+}, determined by Equation 20 and representing an abiotic system, was found to be 2.86 d at pH 5.5, 286 d at pH 4.5, and 3740 d at pH 1.45. This indicated that the abiotic oxidation of Fe^{2+} with O_2 was extremely pH sensitive. The reaction was rapid above pH 5, and became extremely slow in very acidic solution. However, in the presence of *T. ferrooxidans*, the halftime was much shorter, even under acidic conditions. It took only 31 and 7.8 min to react 50% of 0.001 M Fe^{2+} in the presence of 1.5 mg and 6.0 mg (dry weight) of *T. ferrooxidans*, respectively (see Reference 117 and references therein).

It is generally accepted that the Michaelis-Menten equation can be used to explain the rate of biological Fe^{2+} oxidation. This was demonstrated by Suzuki et al.,[144] who studied the oxidation of Fe^{2+} to Fe^{3+} with O_2 by various strains and cell concentrations of *T. ferrooxidans*. They found that the Michaelis-Menten constant (K_m) values remained the same at different cell concentrations of laboratory strains but increased with increasing cell concentrations of mine isolates. They suggested that competitive inhibition of the Fe^{2+}-binding site of a cell by other cells in the reaction mixture explained the behavior of the mine isolates.

As pointed out above, bacteria play a very important role in pyrite oxidation through oxidation of Fe^{2+} to Fe^{3+}, a strong pyrite oxidant. For this reason, pyrite oxidation kinetics are strongly linked to Fe^{2+} oxidation,[76] and bacterial activity. Jaynes et al.[76] reviewed and summarized the conditions under which *T. ferrooxidans* activity is optimized. The data in Figure 3 show that the optimum temperature for *T. ferrooxidans* is around 30°C. Bacterial activity diminishes greatly above and below that temperature, reaching a minimum at approximately 5 and 55°C, respectively.

The data in Figure 4 show that *T. ferrooxidans* (obligate aerobes) activity ceases when O_2 is depleted. However, bacterial activity resumes even under extremely small increases in O_2 content and reaches a maximum at approximately 0.01 mol fraction O_2 or 1%. Finally, the influence of pH on *T. ferrooxidans* is shown in Figure 5. Maximum activity is reached around pH 3.2, whereas minimum activity is reached at approximately pH 1.5 and 5. Jaynes et al. [76]linked pH-dependent activity to pyrite oxidation by the fact that at a pH below 2.5, bacteria physiological limitations diminish their potential in producing Fe^{3+}, whereas above pH 3.5, the pyrite oxidation rate is limited by the decreasing solubility of $Fe(OH)_3$.

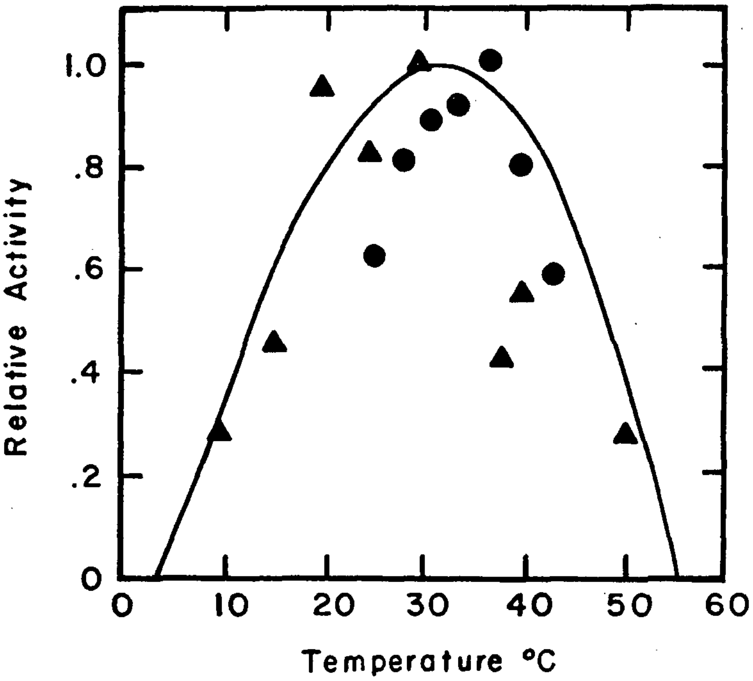

FIGURE 3. Influence of temperature on relative activity of *T. ferrooxidans*. (After Jaynes, D. B., Rogowski, A. S., and Pionke, H. B., *Water Resour. Res.*, 20, 233, 1984, and references therein.)

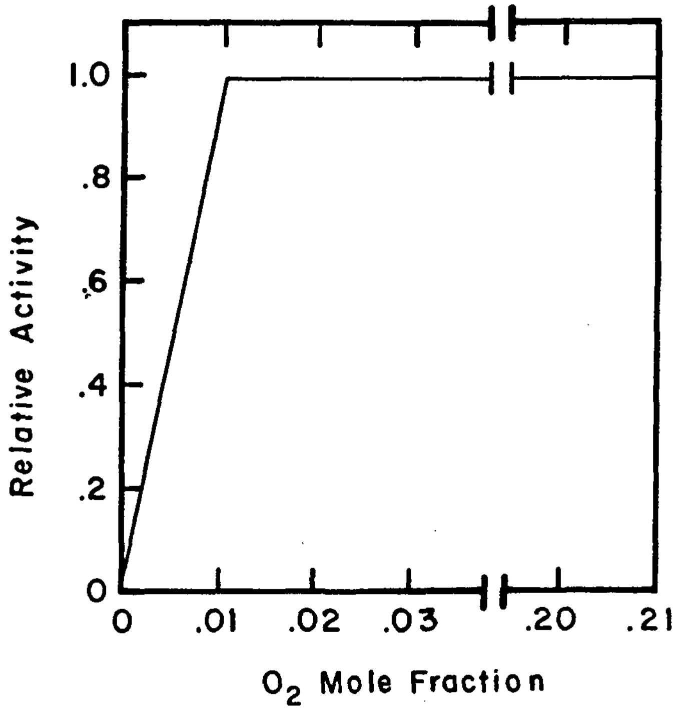

FIGURE 4. Influence of O_2 concentration on relative activity of *T. ferrooxidans* . (After Jaynes, D. B., Rogowski, A. S., and Pionke, H., B. *Water Resour. Res.*, 20, 233, 1984, and references therein.)

The influence of pH and temperature on pyrite oxidation as predicted by Jaynes et al.[76] is demonstrated in Figures 6 and 7. The data in Figure 6 show pyrite oxidation progress in mine waste at 21°C and pH 3 (maximum bacterial activity) in the presence and absence of bacteria. It is clearly shown that bacteria catalyzed pyrite oxidation. The data in Figure 7 show pyrite oxidation progress in mine waste at 6°C and pH 3. These data show that after 40 d, the rate of pyrite oxidation was the same in the presence or absence of bacteria. These observations demonstrate that bacterial activity is indeed temperature dependent and involved in pyrite oxidation. Note that the pyrite oxidation rate (Figure 6) is much greater under optimum conditions for bacterial activity than that under limiting conditions of bacterial activity (Figure 7).

Based on the above information, pyrite oxidation is greatly reduced at pH above 4.5. For this reason, limestone application in the field for controlling pyrite oxidation is recommended. However, evidence shows that pyrite oxidation accelerates at pH values near neutral to alkaline. The mechanisms of this process are discussed in the following sections.

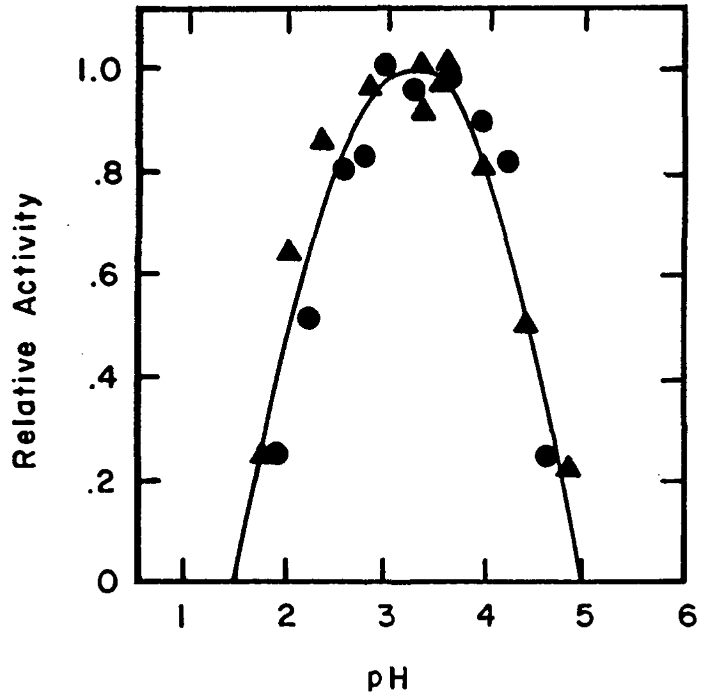

FIGURE 5. Influence of pH on relative activity of *T. ferrooxidans*. (After Jaynes, D. B., Rogowski, A. S., and Pionke, H., B. *Water Resour. Res.*, 20, 233, 1984, and references therein.)

3. Effect of Anions on Oxidation of Fe^{2+}

Abiotic oxidation of Fe^{2+} is affected differently by various anions often present in natural water, such as OH^-, HCO_3^-, Br^-, NO_3^-, ClO_4^-, Cl^-, SO_4^{2-} and $B(OH)_4^-$. Millero[101] indicated that the second–order pyrite oxidation dependence on $[OH^-]$ (see Equation 20) can be attributed to the following rate-determining step

$$\begin{aligned} &Fe(II)(H_2O)_5OH_2 \\ &+1/2O_2 \rightarrow Fe(III)(H_2O)_5(OH)^{2+} + O^{2-} + OH^- \end{aligned} \tag{22}$$

The O^{2-} radical formed as shown in Reaction 22 quickly reacts with Fe^{2+} or $Fe(II)(H_2O)_5(OH)^+$. Goto et al.[60] proposed a reaction scheme in which $Fe(II)(H_2O)_5(OH)^+$ reacted with hydrolyzed molecular oxygen (O_2OH^-) to form a transition complex with only one Fe(III), as shown below in Equation 23

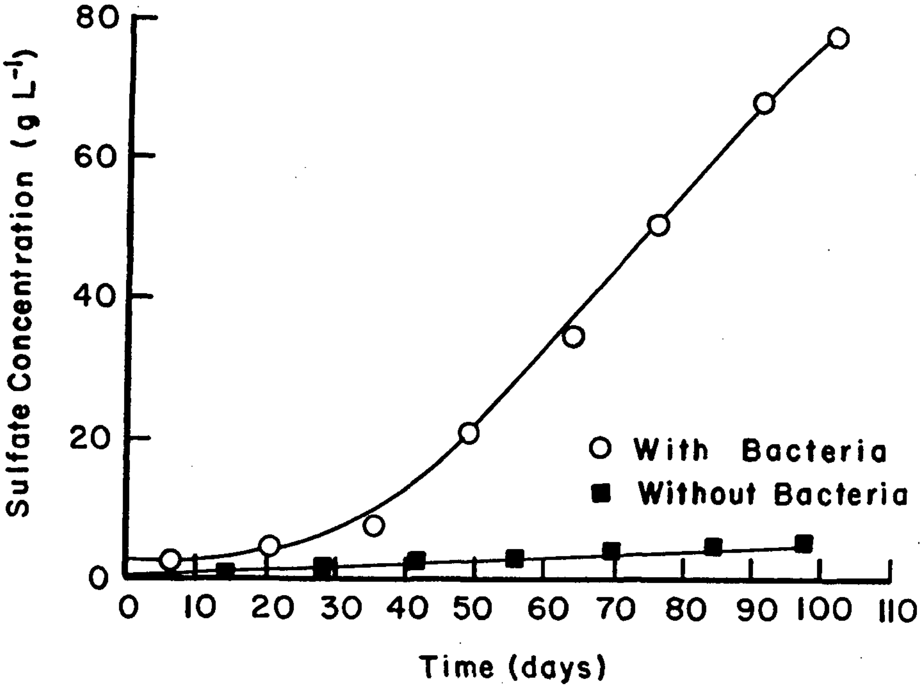

FIGURE 6. Pyrite oxidation kinetics in mine waste at 21 °C and pH 3 in the presence and absence of bacteria. (After Scharer, J. M., Garga, V., Smith, R., and Halbert, B. E., in The Second National Conference on the Abatement of Acidic Drainage, Vol. 2, Montreal, Canada, September 16 to 18, 1991, 211.)

$$\begin{aligned}&\mathrm{Fe(II)(H_2O)_5OH^+}\\&+\mathrm{O_2OH^-}\rightarrow\mathrm{Fe(III)(H_2O)_5(OH)O_2}+\mathrm{O^{2-}}+\mathrm{H_2O}\end{aligned}\tag{23}$$

Millero and Izaguirre[102] also suggested that the second-order Fe^{2+} oxidation dependence on $[OH^-]$ apparently was due to the greater reactivity of $Fe(II)(H_2O)_5(OH)^+$. However, Reactions 22 and 23 are unlikely to take place because superoxide (O^{2-}) may not be an oxygen reduction intermediate in Fe^{2+} oxidation.[102] Millero and Izaguirre.[102] investigated the oxidation of aqueous Fe^{2+} at circumneutral pH and in the absence of ligands (other than H_2O, OH^-, and Cl^-) and in the absence of catalysts (e.g., microbes or solid surface). Their kinetic evidence suggested that Fe^{2+} and dissolved oxygen react in a transition state complex; the reaction produces hydrogen peroxide, which oxidizes Fe^{2+}.

Millero and Izaguirre[102] examined the effect various other anions have on the abiotic oxidation rate of Fe^{2+} at constant ionic strength ($I = 1.0$) and found that this

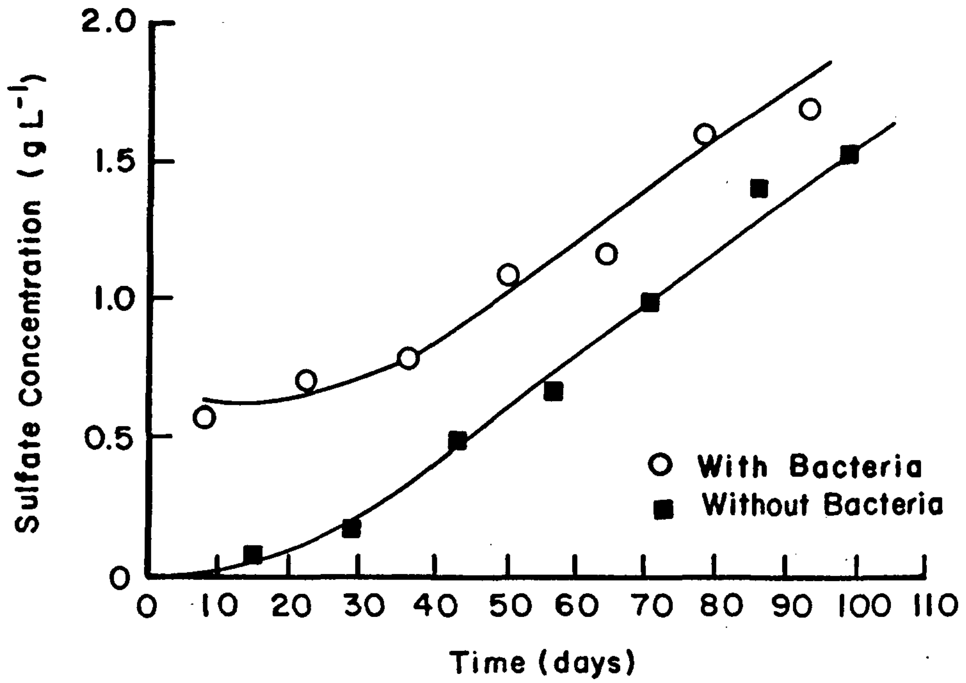

FIGURE 7. Pyrite oxidation kinetics in mine waste at 6 °C and pH 3 in the presence and absence of bacteria. (After Scharer, J. M., Garga, V., Smith, R., and Halbert, B. E., in The Second National Conference on the Abatement of Acidic Drainage, Vol. 2, Montreal, Canada, September 16 to 18, 1991, 211.)

effect was on the order: $HCO_3^- > Br^- > NO_3^- > ClO_4^- > Cl^- > SO_4^{2-} > B(OH)_4^-$. The strong decrease in the rate of Fe^{2+} oxidation due to the addition of SO_4^{2-} and $B(OH)_4^-$ pairs was attributed to the formation of $FeSO_4^0$ and $Fe[B(OH)_4]^+$ pairs, which they assumed were difficult to oxidize. They also reported that the oxidation of Fe^{2+} is first-order with respect to HCO_3^-. This HCO_3^- dependence of Fe^{2+} oxidation could be related to the formation of the $FeHCO_3^+$ pair, which has a faster rate of oxidation than the $Fe(OH)_2^0$ pair. The change in the rate of oxidation of Fe^{2+} due to OH^-, F^-, $H_2PO_4^-$, and HCO_3^- has important implications in the kinetics of pyrite oxidation in neutral to alkaline conditions.

E. Mechanisms of Pyrite Oxidation by Fe^{3+} and Dissolved O_2

According to Singer and Stumm,[129] Fe^{3+} is the major pyrite oxidant in the acidic pH region, while O_2 is expected to be the direct pyrite oxidant at neutral to alkaline pH. The essential feature of the above reaction mechanisms (low or high pH) is initiation of pyrite oxidation by adsorption of O_2 onto a partially protonated pyrite surface.[57] However, recent investigations of pyrite oxidation carried out by Moses et al.,[106] Moses and Herman[105] and Brown and Jurinak[20] demonstrated that Fe^{3+} may be a very effective oxidant at circumneutral pH. The conclusion that Fe^{3+} could be the major direct pyrite oxidant at circumneutral pH was supported by theoretical considerations based on magnetic properties or a molecular orbital theory of the reactants involved.[95–97,106] Moses et al.[106] pointed out that there was a low probability for a direct reaction between paramagnetic molecular O_2 and diamagnetic pyrite. The transfer of a hydroxyl radical from the $Fe(H_2O)_5(OH)^{2+}$ complex to S_2^{2-} however, overcomes a similar restriction on the reaction between Fe^{3+} and pyrite. The experimental results of Moses et al.[106] indicated that pyrite oxidation over a pH range of 2 to 9 was favored in the presence of Fe^{3+} as opposed to dissolved O_2, and that a low concentration of Fe^{3+} was very effective in oxidizing pyrite.

Luther[96] explained that the faster rate of pyrite oxidation by Fe^{3+} was due to the fact that Fe^{3+} can bind chemically to the pyrite surface, whereas O_2 cannot. Access of O_2 to the surface of pyrite, attributed to physical adsorption, has been pointed out by Goldhaber[57] and Mckibben and Barnes.[98] The difference in binding between Fe^{3+} and O_2 with the pyrite surface can be explained on the basis of molecular orbital theory. It turns out that because Fe^{3+} has a vacant orbital, it binds to the pyrite surface via sulfur to form a persulfido bridge ($Fe–S–S–Fe(H_2O)_5(OH)^{2+}$, a transition state intermediate. Through this bridge an electron can be transferred from the highest occupied molecular orbital of S_2^{2-} to the lowest unoccupied molecular orbital of Fe^{3+}. Unlike Fe^{3+}, O_2 cannot form a transition state intermediate with the pyrite surface. This Fe^{3+} pyrite oxidation mechanism, suggested by Luther,[96] is also consistent with the following well-known experimental observations: (1) sulfoxy species ($S_2O_3^{2-}$) are intermediates produced during the process of pyrite oxidation by either Fe^{3+} or O_2, (2) O_2 does not oxidize $S_2O_3^{2-}$ as readily as Fe^{3+} so that when O_2 is the sole pyrite, oxidant sulfoxy compounds are more prevalent, and (3) water is the source of oxygen for the sulfoxy intermediates or sulfate (the latter have been demonstrated experimentally by Taylor et al.,[145,146] employing oxygen isotopes).

Considering that electron transfer reactions are limited to only one or two electron transfer events, Luther[96] proposed a molecular orbital (MO) inner transfer pyrite oxidation mechanism, assuming that this electron transfer would take place in a symmetrical fashion. This involves the transfer of electrons from the highest occupied molecular orbital (HOMO) of the reductant (FeS_2) to the lowest unoccupied molecular orbital (LUMO) of the oxidant (e.g., Fe^{3+}). The process requires that all electron transfers would involve the reduced sulfur of pyrite and the pyrite-surface adsorbed oxidant; thus, no electron transfer would take place between pyrite structural Fe^{2+} and oxidant. The MO model proposed by Luther[96] is consistent with the pyrite oxidation data of Moses et al.,[106] Goldhaber,[57] Mckibben and Barnes,[98] Wiersma and Rimstidt,[157] and the model proposed by Moses et al.[106] and more recently by Moses and Herman.[105]

The molecular structure of pyrite can be represented as:[95]

$$\mathrm{Fe(II)} - \overline{\underline{S_A}} - \overline{\underline{S_B}}\,\Big| \tag{24}$$

Based on frontier-molecular-orbital theory as described by Luther, [95]the surface exposed S_B in the pyrite structure possesses an unshared pair of electrons. This S_B unshared pair of electrons produces a slightly negatively charged pyrite surface that can attract molecules or cations willing to share the pair of electrons. Clearly, preference would be given to those ions or molecules acting as Lewis acids (willing to accept the unshared pair of electrons from S_B). Compounds or ions that could accept this pair of electrons fall into three broad categories: (1) metallic transitional cations (e.g., Fe^{2+}, Fe^{3+}, Cr^{2+}, etc.), (2) molecular halogens (e.g., F_2, Cl_2, I_2, and Br_2, and (3) singlet or light-activated oxygen ($^1O_2$) and H_2O_2. [95]

As pointed out previously, the literature clearly shows that the major pyrite oxidant (electron acceptor) in biotic and abiotic natural systems is Fe^{3+}.[57,98,106,129,157] Luther[96] described the oxidation of pyrite by Fe^{3+} in three major steps. The first step involves the removal of a water ligant from $Fe(H_2O)_6^{3+}$ or its hydrolysis product $[Fe(H_2O)_5(OH)]^{2+}$.

$$\mathrm{Fe(H_2O)_6^{3+}} \rightarrow \mathrm{Fe(H_2O)_5^{3+}} + \mathrm{H_2O} \tag{25}$$

In the second step, the coordinately unsaturated $Fe(H_2O)_5^{3+}$ species can bind to the surface of pyrite through S_B, forming a persulfido bridge. The latter is defined as two metals sharing a common ligand. In this case, the pyrite structural Fe^{2+} and the $Fe(H_2O)_5^{3+}$ share the disulfide ($-S_2^{2-}$).

$$\mathrm{Fe(II)} - \overline{\underline{S_A}} - \overline{\underline{S_B}} - \mathrm{Fe(H_2O)_5^{3+}} \tag{26}$$

In the third step, a symmetrical electron transfer or electron transfer within similar molecular bonding orbitals takes place, and the following pyrite surface radical is formed

$$\begin{gathered}\mathrm{Fe(II)} - \overline{\underline{S_A}} - \overline{\underline{S_B}} - \mathrm{Fe(H_2O)_5^{3+}} \rightarrow \\ \mathrm{Fe(II)} - \overline{\underline{S_A}} - \underline{\overset{+}{\dot{S}}_B} - \mathrm{Fe(H_2O)_5^{2+}}\end{gathered} \tag{27}$$

The product of Reaction 27 reacts with $Fe(H_2O)_6^{3+}$ and H_2O to transfer a second electron to $Fe(H_2O)_6^{3+}$ and one oxygen atom from H_2O to the pyrite surface (Taylor et al., 1984a,b). In the process, two H^+ and a S_2O are produced as follows:

$$\begin{aligned}&\mathrm{Fe(II)}-\overline{\underline{\mathrm{S}_\mathrm{A}}}-\underline{\overset{+\cdot}{\mathrm{S}}_\mathrm{B}}-\mathrm{Fe(H_2O)_5^{2+}}\\&+\mathrm{Fe(H_2O)_6^{3+}}+\mathrm{H_2O}\rightarrow\\&\quad\mathrm{Fe(II)}-\overline{\underline{\mathrm{S}_\mathrm{A}}}-\overline{\underline{\mathrm{S}_\mathrm{B}}}-\overline{\underline{\mathrm{O}}}|+2\mathrm{Fe(H_2O)_6^{2+}}+2\mathrm{H^+}\end{aligned}\tag{28}$$

Pyrite electron transfer continues until iron thiosulfate (FeS_2O_3) formation and detachment from the pyrite surface is completed. Reaction 29 reveals the transfer of two additional electrons, while Reaction 30 shows the transfer of the final two electrons, leading to $S_2O_3^{2-}$ formation

$$\begin{aligned}&\mathrm{Fe(II)}-\overline{\underline{\mathrm{S}_\mathrm{A}}}-\overline{\underline{\mathrm{S}_\mathrm{B}}}-\overline{\underline{\mathrm{O}}}+2\mathrm{Fe(H_2O)_6^{3+}}+\mathrm{H_2O}\rightarrow\\&\quad\mathrm{Fe(II)}-\overline{\underline{\mathrm{S}_\mathrm{A}}}-\underline{\underline{\overset{\overline{|\mathrm{O}|}}{\overset{|}{\mathrm{S}}}_\mathrm{B}}}-\overline{\underline{\mathrm{O}}}|+2\mathrm{Fe(H_2O)_6^{2+}}+2\mathrm{H^+}\end{aligned}\tag{29}$$

and

$$\begin{aligned}&\mathrm{Fe(II)}-\overline{\underline{\mathrm{S}_\mathrm{A}}}-\underline{\overset{\overline{|\mathrm{O}|}}{\overset{|}{\mathrm{S}}}_\mathrm{B}}-\overline{\underline{\mathrm{O}}}|+2\mathrm{Fe(H_2O)_6^{3+}}+\mathrm{H^2O}\rightarrow\\&\quad\mathrm{Fe(II)}-\overline{\underline{\mathrm{S}_\mathrm{A}}}-\underset{\underline{|\mathrm{O}|}}{\underset{|}{\overset{\overline{|\mathrm{O}|}}{\overset{|}{\mathrm{S}_\mathrm{B}}}}}-\overline{\underline{\mathrm{O}}}|+2\mathrm{Fe(H_2O)_6^{2+}}+2\mathrm{H^+}\end{aligned}\tag{30}$$

Finally, surface-product detachment produces solution iron thiosulfate (Fe^{II} + $S_2O_3^{2-}$)

Based on the above reactions, two electron transfer mechanisms account for the pyrite–surface oxidation process: formation of a surface free radical (Reaction 27) and transfer of an oxygen atom from the water molecule to S_B (Reaction 28).[145,146] Each one of the mechanisms is responsible for the transfer of three electrons, for a total of six. Moses et al.[106] and Brown and Jurinak[19,20] postulated that three of the electrons are transferred through an OH^- bridging ligand between Fe^{3+} and the pyrite surface, while the remaining three electrons are transferred by the removal of H^+ from $Fe–S_A–S_B–OH$ by formation of H_2O. The OH^- bridging ligand between Fe^{3+} and the pyrite surface appears to account for the large increase in pyrite oxidation observed at pH values above 7[19,20,57] (Figure 8).

Summarizing reactions 26 through 30 gives

$$\begin{aligned}&\mathrm{FeS_2}+6\mathrm{Fe(H_2O)_6^{3+}}+3\mathrm{H_2O}\rightarrow\\&\quad\mathrm{Fe^{2+}}+\mathrm{S_2O_3^-}+6\mathrm{Fe(H_2O)_6^{2+}}+6\mathrm{H^+}\end{aligned}\tag{31}$$

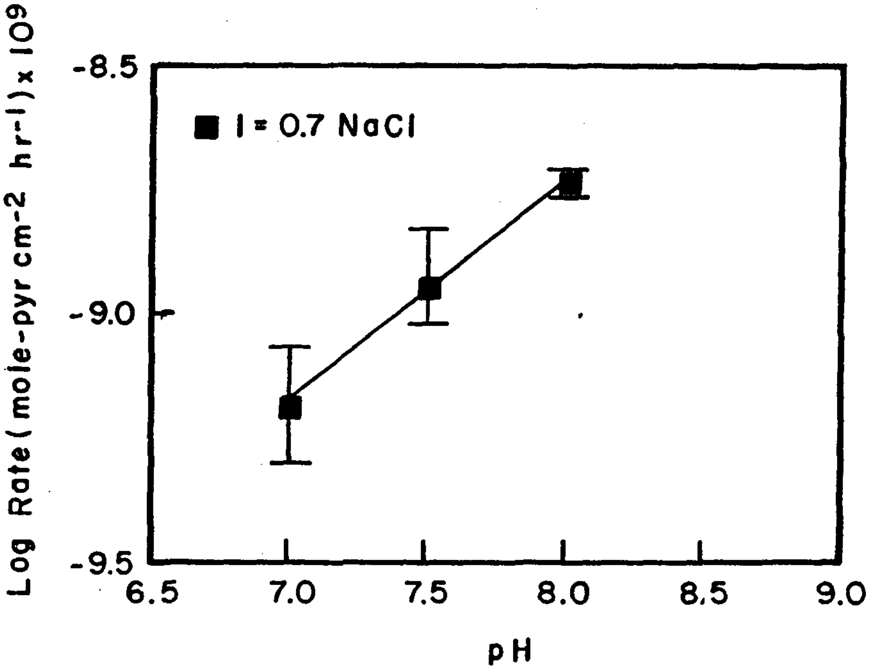

FIGURE 8. Kinetics of pyrite oxidation as influenced by pH. (After Hood, T. A., The Kinetics of Pyrite Oxidation in Marine Systems, Ph.D. thesis, University of Miami. Coral Gables, FL, 1991.)

Therefore, the transfer of six electrons from S_B to six Fe^{3+} produces one $S_2O_3^{2-}$ and six H^+. In the presence of excess Fe^{3+}, $S_2O_3^-$ is rapidly transformed to SO_4^{2-} according to Reaction 32.

$$5H_2O + S_2O_3^{2-} + 8Fe^{3+} \rightarrow 8Fe^{2+} + 10H^+ + 2SO_4^{2-} \qquad (32)$$

Summation of Reactions 31 and 32 produces Reaction 33.

$$8H_2O + FeS_2 + 14Fe^{3+} \rightarrow 15Fe^{2+} + 16H^+ + 2SO_4^{2-} \qquad (33)$$

Data in the literature substantiate that $S_2O_3^{2-}$ in the presence of a strong oxidizer (e.g., Fe^{3+} or H_2O_2) rapidly oxidizes to sulfate (SO_4).[95] In fact, Luther[95] pointed out that the oxidation of $S_2O_3^{2-}$ or sulfite (SO_3^{2-}) by Fe^{3+} or H_2O_2 is rapid enough that such products would not be detected in solution. Moses et al.[106] carried out pyrite oxidation experiments and specifically focused on evaluating the production of SO_3^{2-}, $S_2O_3^{2-}$ and $S_nO_6^{2-}$. The results of their study revealed that none of the above sulfoxy anions were detected when the oxidant was Fe^{3+}. However, when the oxidant was dissolved oxygen, significant quantities of sulfoxy anions (SO_3^{2-}, $S_2O_3^{2-}$ and $S_nO_6^{2-}$) were produced at a pH greater than 3.9. Similar observations were made by Taylor et al.[145,146] Their investigations involved laboratory and field studies, and the authors reported that no sulfoxy anion species were detected.

The limiting step in the oxidation of pyrite is oxidation of Fe^{2+} by dissolved O_2.

$$Fe(H_2O)_6^{2+} + 1/4O_2 + H^+ \rightarrow Fe(H_2O)_6^{3+} + 1/2H_2O \qquad (34)$$

According to Moses et al.[106] and Moses and Herman,[105] Fe^{3+} is an effective and direct pyrite oxidant at low pH, as well as at circumneutral pH and the role played by dissolved O_2 is to sustain the reaction by regenerating Fe^{3+}. For additional details on this model, see Moses and Herman.[105] It is well known that the rate of Fe^{2+} oxidation increases as pH increases.[102,129] The role of OH^- in oxidizing Fe^{2+} has been postulated by Luther et al.[97] to be due to the potential increase in the frontier molecular orbital electron density of Fe^{2+} after binding to oxygen by coordinating OH^-. Such coordination increases Fe^{2+} basicity and stabilizes the Fe^{3+} formed. Luther et al.[97] demonstrated that an increase in electron density also increases the potential of Fe^{2+} to oxidize rapidly to Fe^{3+} when the former (Fe^{2+}) is in the form of a complex with a ligand containing oxygen as the ligating atom. The above, according to Luther et al.,[97] also explains the observed increase in pyrite oxidation as pH increases or as soluble Fe^{3+}–organic complexes increase, especially if the latter is positively charged and less stable than the Fe^{2+}–organic complex.

F. Pyrite Surface Chemistry

Pyrite/surface exposed S_B (Reaction 24) provides a slightly negatively charged pyrite surface due to an unshared pair of electrons that attract ions willing to share them (e.g., Fe^{2+}). However, the relatively low negative pyrite/surface charge cannot fully compensate for the positive charge of Fe^{2+}; for this reason, Evangelou and Huang[49] postulated that pyrite/surface–adsorbed Fe^{2+} reacts with CO_3^{2-} to form a pyrite/surface Fe(II)–CO_3 complex of a certain configuration (e.g., bidentate, unidentate, or electrostatic as shown below.

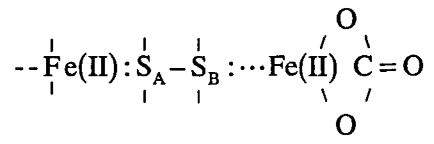

$$--\mathrm{Fe(II)}:\mathrm{S_A}-\mathrm{S_B}:\cdots\mathrm{Fe(II)}\ \overset{\mathrm{O}}{\underset{\mathrm{O}}{\mathrm{C}}}=\mathrm{O} \qquad (35)$$

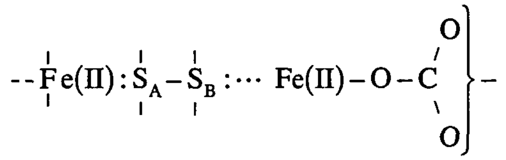

$$--\mathrm{Fe(II)}:\mathrm{S_A}-\mathrm{S_B}:\cdots\ \mathrm{Fe(II)}-\mathrm{O}-\left.\overset{\mathrm{O}}{\underset{\mathrm{O}}{\mathrm{C}}}\right\}- \qquad (36)$$

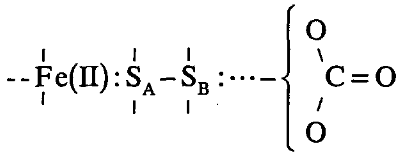

$$\text{--}\overset{|}{\underset{|}{\text{F}}}\text{e(II)}:\overset{|}{\underset{|}{S}}_A-\overset{|}{\underset{|}{S}}_B:\cdots-\left\{\begin{array}{l}O\\ \;\backslash\\ \;\;C=O\\ \;/\\ O\end{array}\right.$$

(37)

Evangelou and Huang[49] carried out a detailed FT-IR pyrite/surface chemistry characterization study employing diffuse reflectance, a highly sensitive spectroscopic surface technique.[5,46] The FT-IR spectra in Figure 9 show that both coal and mineral pyrites exhibit a strong infrared absorption band around 440 cm. This vibrational band is assignable to the disulfide (S-S) in the pyrite lattice,[70] but does not seem to occur at the same exact wavenumber on all samples; it may suggest structural differences between pyrites. Pyrite samples 1 and 2 represent well-crystallized massive pyrites, while the coal pyrite sample represents framboidal and most likely poorly crystallized pyrite.[49]

Pyrite is known to be extremely sensitive to exposure to atmospheric air. This may explain the spectra behavior of pyrite below the 1200-cm range after hydrofluoric acid (HF) wash, to remove any surface impurities, and evacuation at 97°C. For example, the spectrum of coal pyrite in Figure 10 exhibits strong absorption at 611 cm. This might result from SO_4^{2-} associated with Fe^{2+} and The broadness of the 611-cm band and in the case of mineral pyrite 1, its apparent splitting into several bands may suggest differences in the amounts and types of sulfoxy anions

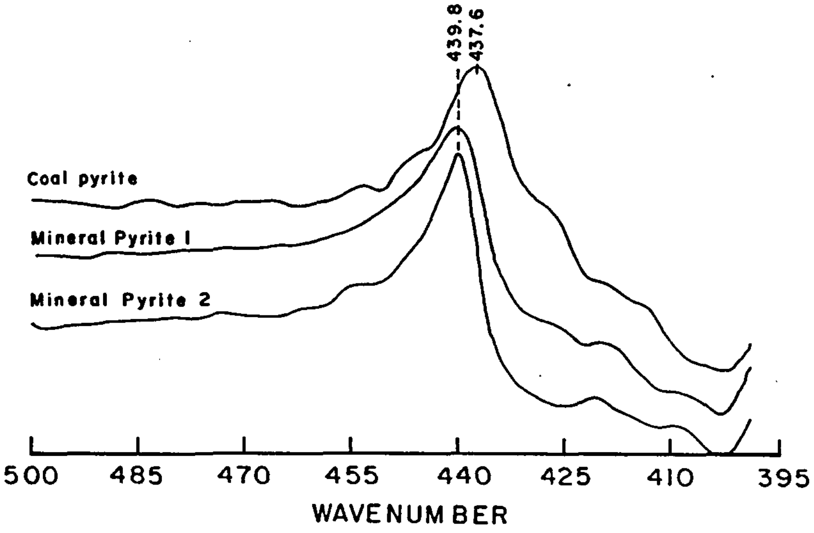

FIGURE 9. FT-IR diffuse reflectance spectra of coal pyrite and mineral pyrites after washing with strong hydrofluoric solution. (After Evangelou, V. P. and Huang, X., *Spectrochim. Acta*, 50A, 1333, 1994.)

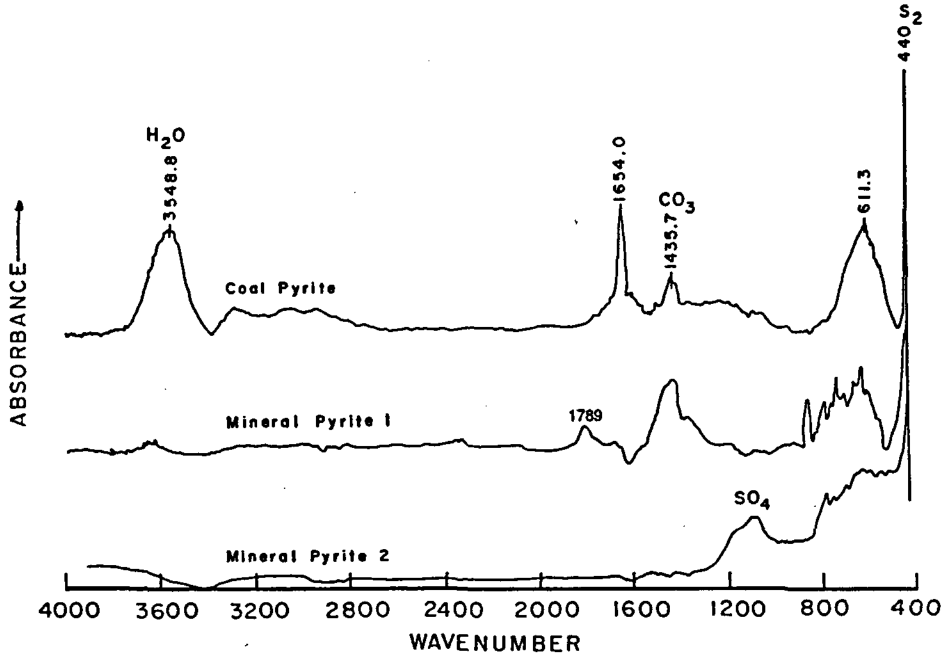

FIGURE 10. FT-IR diffuse reflectance spectra of coal pyrite and mineral pyrites after washing with strong hydrofluoric solution. (After Evangelou, V. P. and Huang, X., *Spectrochim. Acta*, 50A, 1333, 1994.)

(e.g., SO_3^{2-}, $S_2O_3^{2-}$ and $S_nO_6^{2-}$) produced under mild oxidizing conditions.[106] These chemical species absorb infrared in the 600-range frequencies. The broad absorption band from 1200 to 900 cm on the spectrum of mineral pyrite 2 suggests the presence of some rapidly forming sulfate associated with Fe^{3+} on the surface of pyrite.[33,34]

The spectra in Figure 10 point out the relative ease with which pyrites oxidize when exposed to air, and that different pyrites oxidize at different rates. Note that the infrared spectra shown in Figure 10 are representative of pyrite samples exposed to air no more than 1 h prior to spectroscopic evaluation. Coal pyrite exhibits a 611-cm band, which most likely represents SO_4^{2-} associated with Fe^{2+}. The same pyrite sample exhibits a CO_3^{2-} band (1430 cm) and a carboxylate (COO^-) band (1560 cm). In the case of mineral pyrite 1, a broad $SO_4^{2-}/S_2O_3^{2-}$ band is observed below 800 cm, as well as a CO_3^{2-} band (1430 cm) and most likely a carbonyl (C=O) band near the 1800 cm range.

The difference in the infrared spectra between coal pyrite and mineral pyrite 1 (Figure 10) is most likely due to differences in the pK_{bs} of the adsorbed carbonate (assuming the same surface pH) or due to differences in surface pH (assuming differences in oxidation rates). Assuming that the pyrite/surface pH of the two pyrites is the same, but their pK_{bs} differ, then the spectra differences with respect to the carboxylate (COO$^-$) and carbonyl (C=O) bands suggest that one surface is deprotonated (coal pyrite) while the other surface (mineral pyrite 1) is protonated. The spectrum of mineral pyrite 2, on the other hand, does not display a CO_3^{2-} band (note the absence of a 1430 cm band), but it does display a SO_4^{2-} band in the 1200 cm range. This band most likely reflects SO_4^{2-} associated with Fe^{3+}.[33,34] It appears that the low surface pH, due to Fe^{3+}, inhibits the formation of surface-adsorbed carbonate. An alternate explanation for the 1430 and 1654 bands of coal pyrite is the direct reaction of CO_2 with S_B as follows:

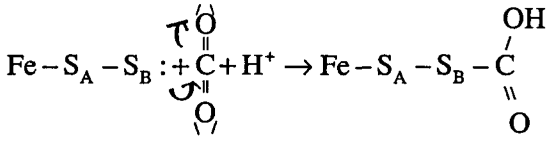

$$\mathrm{Fe-S_A-S_B:+\underset{\underset{\displaystyle O}{\|}}{\overset{\overset{\displaystyle O}{\|}}{C}}+H^+ \rightarrow Fe-S_A-S_B-\underset{\underset{\displaystyle O}{\backslash\backslash}}{\overset{\overset{\displaystyle OH}{/}}{C}}} \qquad (38)$$

The above reaction product could exhibit infrared absorption bands similar to those of CO_3^{2-} coordinated by pyrite/surface-adsorbed Fe^{2+}. In other words, one would be able to observe C–O symmetric vibrations at around 1430 cm, carbonyl (C=O) vibrations at about 1750 cm, and carboxylate vibrations at about 1560 cm.[67] The exact wavenumbers of these vibrations would depend on the nature of the sulfur-carbon bond. Some support for the above-postulated pyrite/surface-CO_2 interactions comes from the pyrite-CO_3 infrared spectroscopic observations reported by Donato et al.[33,34] The importance of these pyrite infrared spectroscopic observations with respect to pyrite oxidation reactions is discussed in the next section.

The spectra in Figure 11 represent mineral pyrite exposed to atmospheric air at 100% relative humidity in a chamber for 14 d. The emergence of absorption bands at 1183.3, 1137, 1097, 980.6, and 608.9 cm clearly indicate the presence of SO_4 on the pyrite surface. The sulfate anion species (SO_4^{2-}) is highly symmetrical, and of four common fundamental vibrations, only v_3 (1200 cm) and v_4 (600 cm) are infrared active. When the symmetry of sulfate is perturbed due to coordination with cations, the degenerate vibrations (v_3) split into a number of distinct vibrations, depending on the strength of the complex, and v_1 vibration is activated. The apparent splitting of v_3 (1183, 1137, and 1097 cm) and the presence of v_1 (980.6 cm) on the spectrum of oxidized mineral pyrite (Figure 11) suggest that sulfate may be bonded to Fe^{3+} in a bindentate fashion.[34] The spectra in Figure 11 also exhibit carbonate absorption bands at 1428 and 867 cm, which are assigned to CO_3 v_3 and v_2 vibrations, respectively

One would assume that the strong acid environment on the surface of pyrite, created by the oxidation of the disulfide, is expected to prevent the formation of Fe(II)–CO_x complexes. However, the persistence of the carbonate absorption band (1430 cm), as shown in Figures 11 and 12, demonstrates that the acid produced could be removed due to its reaction with pyrite as follows:[49]

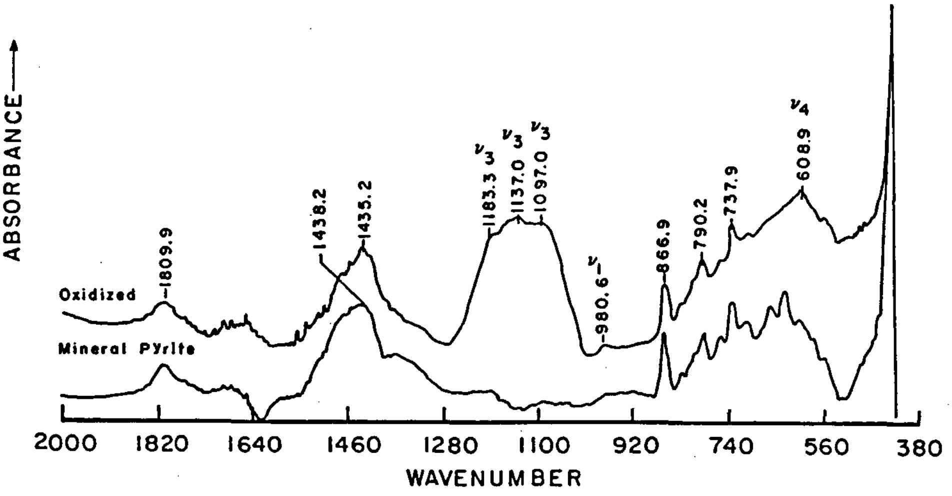

FIGURE 11. FT-IR diffuse reflectance spectra of mineral pyrite 1 (Peru pyrite) after oxidation by O_2 at 100% relative humidity. (After Evangelou, V. P. and Huang, X., *Spectrochim. Acta*, 50A, 1333, 1994.)

$$FeS_2 + H_2SO_4 = FeSO_4 + H_2S + S^o \qquad (39)$$

In Reaction 39, it is suggested that protons are removed during H_2S volatilization after placing the pyrite sample under vacuum on any other O_2-consuming conditions. Therefore, after oxidation, the surface of pyrite is most likely covered with a layer of ferrous sulfate and S^o, and most active anodic sites (S_B) are saturated with Fe^{2+}.[57,105]

The infrared absorption band near 1621 cm shown in Figure 12 is assigned to the H_2O deformation band. The band at 1650 cm suggested the presence of an additional pyrite/surface chemical species. When the oxidized mineral pyrite was exposed to desiccation at room temperature, and heated to 160°C for 4 h and 8 h under a nitrogen gas atmosphere, the absorption band at 1650 cm decreased in intensity, while the 1621-band and the 1430-cm bands remained intact. This suggested that the 1621-cm absorption band was most likely due to carboxylate (COO^-). When the pyrite sample was heated, adsorbed water decreased and, therefore, surface acidity increased, leading to carboxylate protonation.[67,103,104] Furthermore, after washing the oxidized pyrite sample with HCl, its spectrum did not exhibit the 1430-cm band, suggesting that the pyrite/surface CO_x ($CO_x = CO_3^{2-}$ or carboxylic species) was removed by the acid. Additionally, the absence of the 1620 cm band, indicative of water loss/absence, could be due to the production of elemental sulfur,[91] a hydrophobic substance.

According to Nakamoto, the extent of splitting (number of distinguishable bands) of the 1430-cm band, representing the free CO_3 ion, could be directly

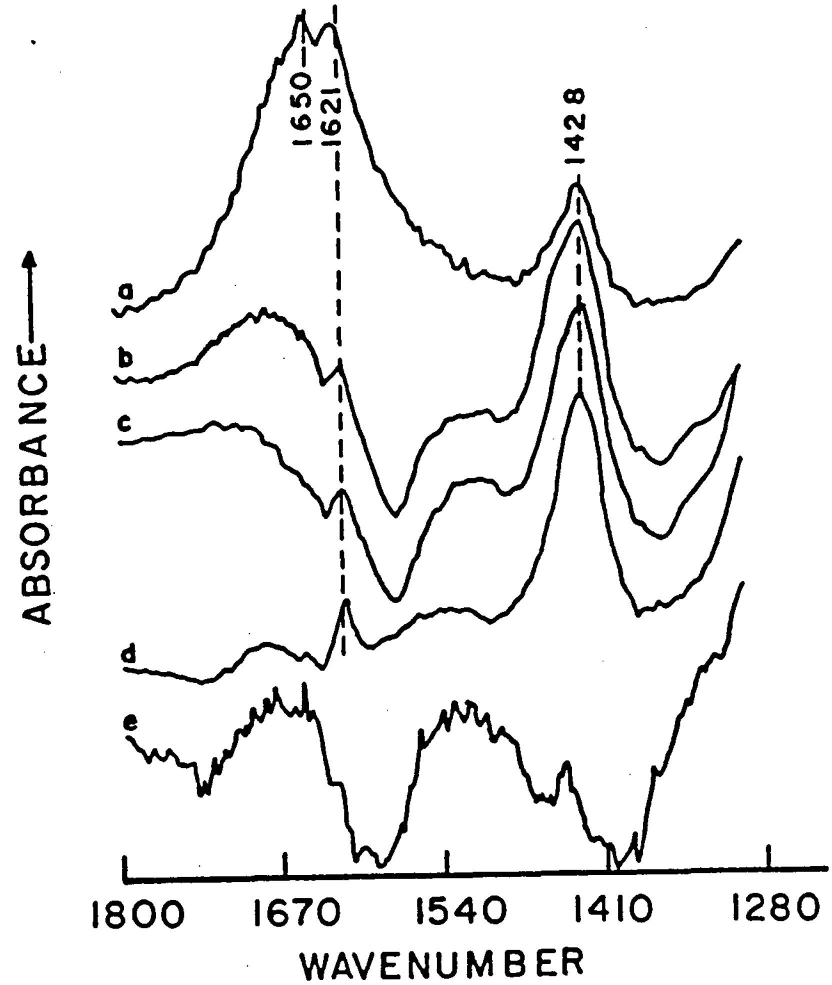

FIGURE 12. FT-IR diffuse reflectance spectra of oxidized mineral pyrite 2 (South Dakota pyrite) after: (a) oxidation, (b) drying in desiccator, (c) heating at 160°C for 3 h, (d) heating at 160°C for 8 h, and (e) washing with 4 *M* HCl. (After Evangelou, V. P. and Huang, X., *Spectrochim. Acta,* 50A, 1333, 1994.)

related to the bond strength between CO_3^{2-} and Fe^{II}. Nonsplitting of the CO_3 band in Figure 12 indicates that pyrite/surface Fe(II)–CO_3 complexes are most likely weak electrostatic complexes (see Reaction 37) or that the 1430-cm band represents the symmetric C–O vibrations of a carboxylic group (see Reaction 38). When the spectrum of bulk $FeCO_3$ is compared with that of $Na_2CO_3^-$ (Figure 13A) or oxidized pyrite (Figure 13B), it is shown that in the case of bulk $FeCO_3$, the 1430-cm band splits into two clearly distinguishable bands, signifying a unidentate complex (see Reaction 36), while in the case of Na_2CO_3 or coal pyrite, the 1430-cm absorption region appears to form more of a single band (Reaction 37, electrostatic

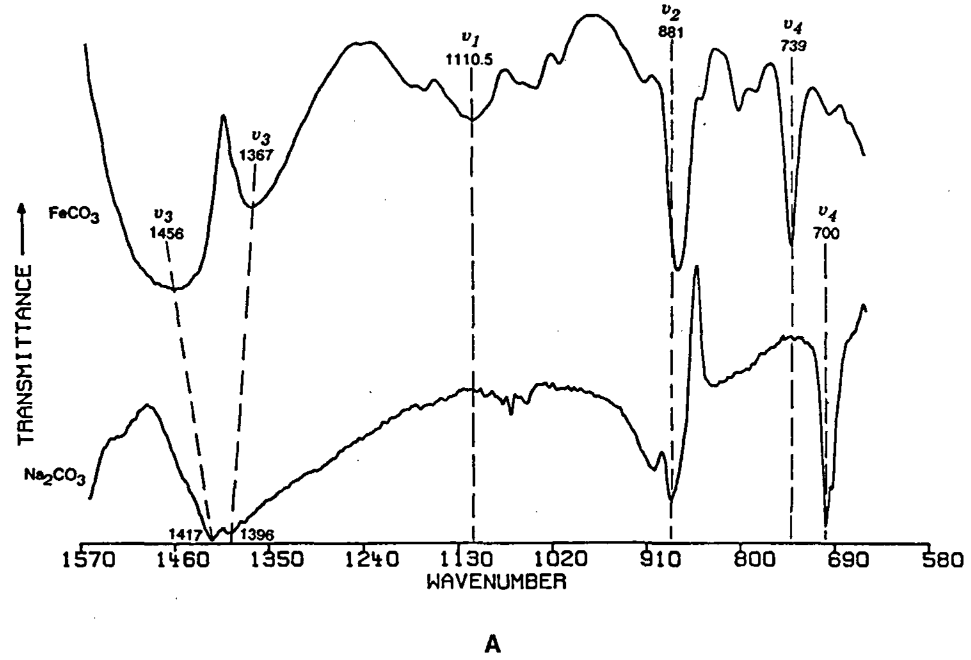

FIGURE 13. (A) FT-IR diffuse reflectance spectra of FeCO$_3$ and Na$_2$CO$_3$. (B) FT-IR diffuse reflectance spectra of FeCO$_3$ and coal pyrite after a several-month exposure to atmospheric air in room temperature. (After Evangelou, V. P. and Huang, X., *Spectrochim. Acta,* 50A, 1333, 1994.)

interaction). Note that Na$_2$CO$_3$ is highly water soluble due to the weak electrostatic attraction between the sodium and carbonate ions.

The above infrared spectra observations are summarized in Figure 14. It shows the symmetric vibrations of CO$_3^{2-}$/COO$^-$ (1430-cm band), the presence of pyrite/surface-adsorbed water (1620 cm), and the vibrations of carbonyl (C=O, 1789-cm band) and carboxylate (COO$^-$, 1681-cm band). Absorption bands in the 3300- to 3600-cm range are also shown; they represent OH$^-$ associated with Fe^{III} and OH associated with pyrite/surface-adsorbed water.

The above infrared spectroscopic evaluation clearly supports the potential adsorption of CO$_2$ by the surface of pyrite either as CO$_3^{2-}$ (weakly adsorbed by pyrite/surface Fe^{II}[57,105]) or as a pyrite surface carboxylic acid group.

Pyrite/surface-CO$_x$ complexes may act as promoters of pyrite oxidation[70] or as precursors to pyrite iron-oxide coatings formation.[111,112] The conditions necessary for forming Fe(II)–CO$_3$ complexes or –COO$^-$ on the surface of pyrite in the absence of carbonate-rich solutions appear to be (1) circumneutral pH and (2) the presence of O$_2$ and CO$_2$ gases. However, further wet chemistry experiments are needed in order to demonstrate the mechanism of promoting pyrite oxidation by Fe(II)–CO$_x$ pyrite/surface complexes or –COO$^-$, and to quantify the conditions,

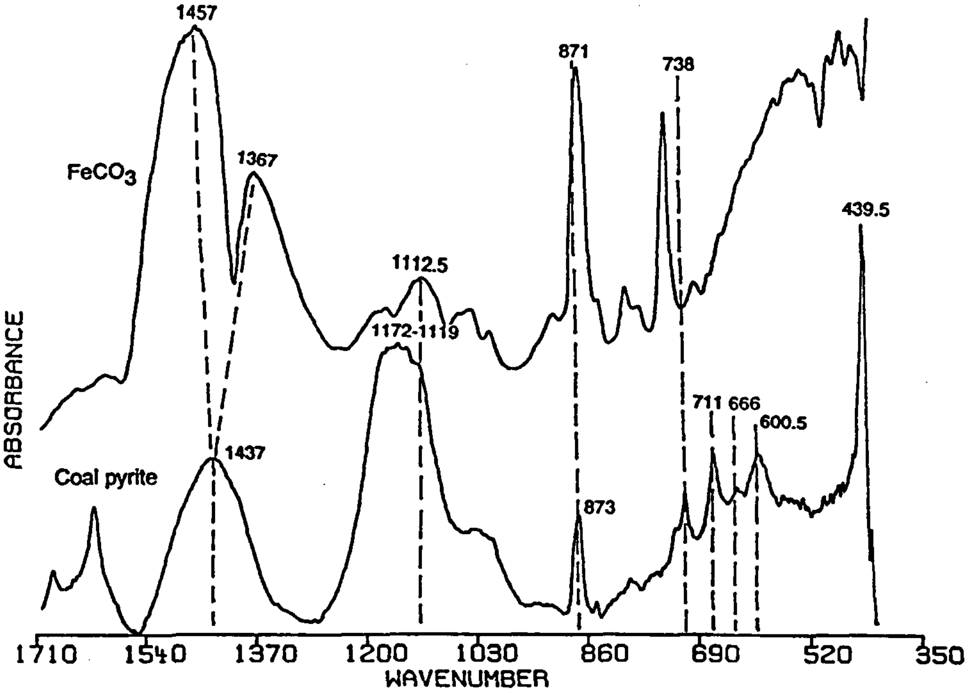

FIGURE 13B

leading to the formation of iron oxide coatings, which may inhibit pyrite oxidation in nature.

G. Pyrite Oxidation and Surface CO_3/CO_2 Reactions

The rates of pyrite oxidation in neutral and alkaline environments (e.g., limestone-buffered sulfide-rich mine wastes) are commonly lower than that in an acidic environment due to the lower solubility of Fe^{3+} and limited bacteria activity. Studies by Nicholson et al.[111,112] indicated that in neutral to alkaline environments, formation of an iron-oxide coating on the pyrite surface can act as pyrite/surface barrier to O_2 or Fe^{3+}, thereby diminishing pyrite oxidation. Nicholson et al.,[111,112] investigating pyrite oxidation kinetics in a bicarbonate-buffered system at pH values between 7.5 and 8.5, observed that the oxidation rate initially increased, reached a maximum at about 400 h, and then decreased to a final, relatively constant lower value (Figure 15). By using X-ray photoelectron spectroscopy and auger electron spectroscopy, the authors found that pyrite particles (215 μm), when oxidized under alkaline conditions, were coated with a ferric oxide coating of approximately 0.6-μm thickness. They concluded that oxide accumulation on the

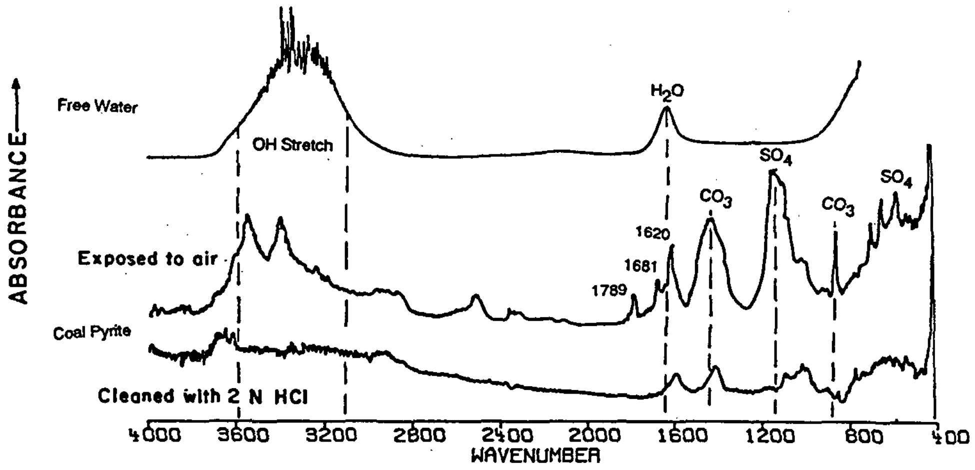

FIGURE 14. FT-IR diffuse reflectance spectra of coal pyrite and mineral pyrite 1 (Peru pyrite) after a several-month exposure to atmospheric air at room temperature. (After Evangelou, V. P. and Huang, X., *Spectrochim. Acta,* 50A, 1333, 1994.)

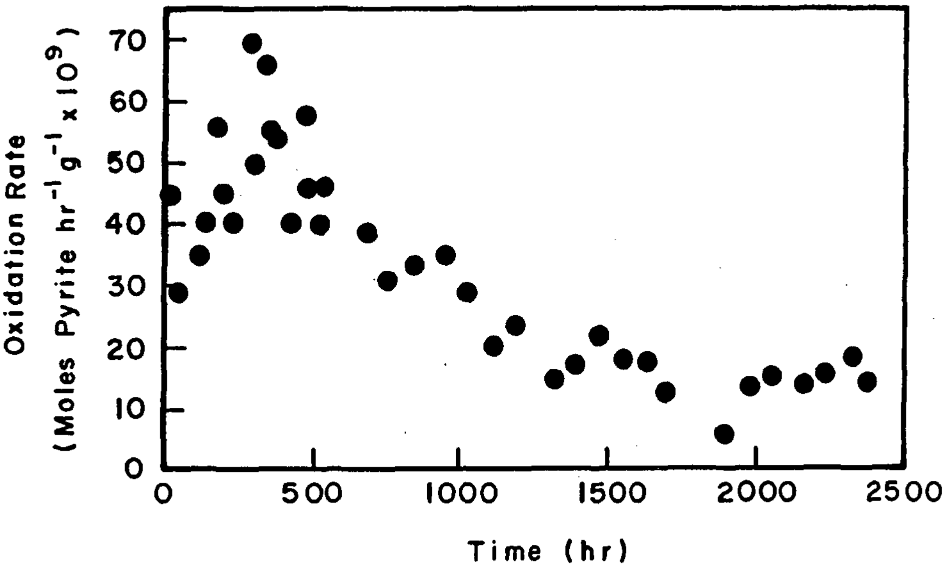

FIGURE 15. Variation in rate of pyrite oxidation in alkaline solutions with time. (After Nicholson, R. V., Gillham, R. W., and Reardon, E. J., *Geochim. Cosmochim. Acta,* 52, 1077, 1988.)

pyrite surface resulted in a significant reduction in the oxidation rate over time. The authors, however, did not investigate the mechanisms by which the ferric iron could be stabilized on the surface of pyrite.

Hood[70] studied the kinetics of pyrite oxidation in alkaline suspensions at a constant pH by maintaining a constant HCO_3^-/CO_3^{2-} ratio and increasing concentration of the two species. Carbonate single-ion activity was varied from 0.002 to approximately 0.05 mmol/l to avoid precipitation of ferrous carbonate in the bulk solution. She observed that the rate of pyrite oxidation increased with increasing carbonate concentration (Figure 16). The same phenomenon may explain the large increase in the pyrite oxidation rate in the presence of $NaHCO_3$ at pH 9, as observed by Brown and Jurinak[19] (Figure 17). Hood[70] concluded that the cause of the observed increase in pyrite oxidation was the formation of a pyrite/surface Fe(II)–CO_3 complex, which facilitated electron transfer to O_2 and consequently rapid oxidation of the ferrous iron. Furthermore, Hood[70] employed her experimental observations to explain the results (involving pyrite oxidation in alkaline solutions) published by Nicholson et al.[112] She concluded that the initial increase in the oxidation rate observed by these authors (Figure 15) was due to pyrite/surface $FeCO_3^0$ complex formation. Hood,[70] further predicted that after oxidation of Fe^{II} of the $FeCO_3^0$ complexes, the complexesform either $Fe(OH)_3(s)$ or FeOOH(s) on the pyrite surface. These iron oxyhydroxide solids accumulate and become a diffusion barrier for the movement of O_2 to the pyrite surface and oxidation

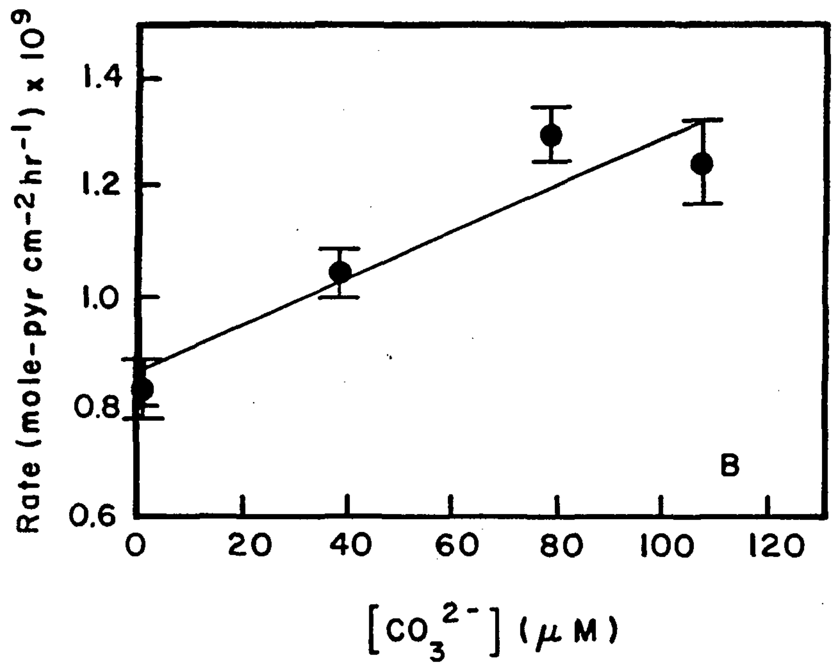

FIGURE 16. Kinetics of pyrite oxidation as influenced by carbonate. (After Hood, T. A., The Kinetics of Pyrite Oxidation in Marine Systems, Ph.D. thesis, University of Miami, Coral Gables, FL, 1991.)

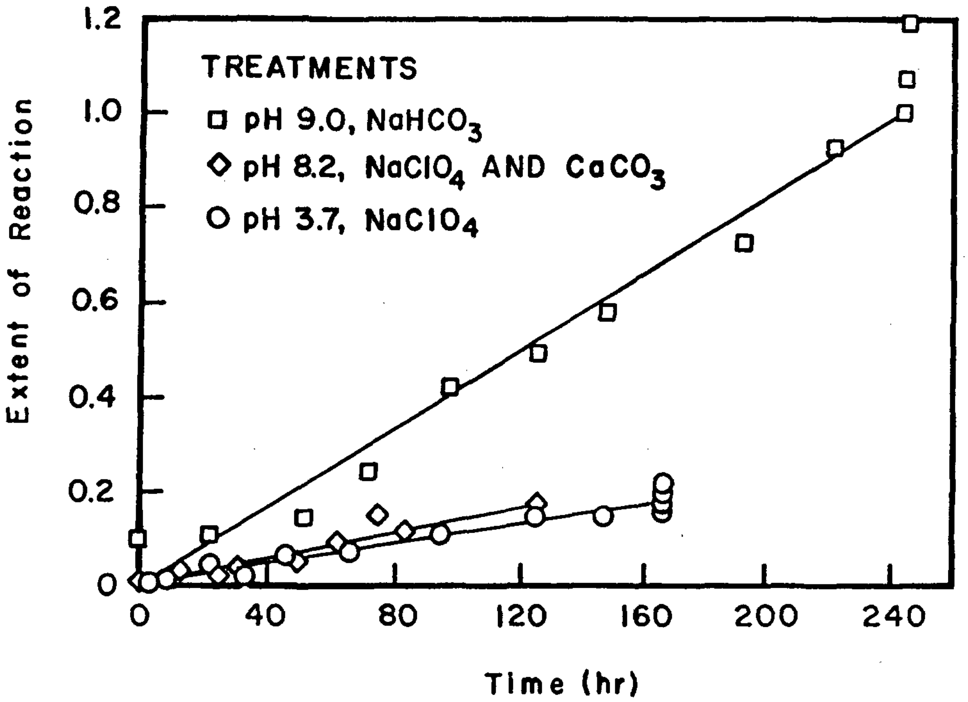

FIGURE 17. Kinetics of pyrite oxidation as influenced by pH. (After Brown, A. D. and Jurinak, J. J., *Arid Soil Res.*, 3, 65, 1989.)

products away from the surface. Due to this barrier, the oxidation rate decreases, eventually reaching the lower value set by the rate of diffusion of reactants and products through the iron oxyhydroxide barrier.

Hood,[70] however, failed to provide direct molecular evidence for the ferrous carbonate complex formed on the pyrite surface. Evangelou and Huang,[49] using FT-IR spectroscopy, demonstrated that pyrite exposure to atmospheric air leads to the formation of pyrite surface Fe(II)–CO_3 complexes and pyrite/surface carboxylic groups that may promote pyrite oxidation by promoting electron transfer, or may act as precursors to pyrite iron-oxide coating formation. FT-IR evidence of CO_3 on the surface of pyrite was also reported by Donato et al., but the carbonate's potential importance to pyrite oxidation was overlooked by these researchers.

Based on (1) experimental observations that at constant pH but an increasing solution CO_3^{2-} concentration, abiotic pyrite oxidation rate increases[19,20,70] and (2) FT-IR spectra supporting the presence of pyrite/surface-CO_3 complexes and pyrite/surface carboxylic groups,[49] the following model is proposed to account for abiotic pyrite oxidation enhancement at a pH near or above neutral in environments enriched with CO_2/CO_3 and O_2.

$$-\mathrm{Fe(H_2O)_5OH^+ + CO_2 \rightarrow Fe(H_2O)_5HCO_3^+} \qquad (40)$$

and

$$\mathrm{Fe(H_2O)_5HCO_3^+ + H_2O + O_2 \rightarrow} \\ \mathrm{-Fe(H_2O)_4(OH)_2^+ + CO_2} \qquad (41)$$

According to Millero and Izaguirre [102], Fe^{2+} oxidation is promoted when in the presence of HCO$_3^-$/CO$_3^{2-}$ due to Fe^{2+}–carbonate complex formation. Luther et al.[97] postulated and then demonstrated that Fe^{2+} complexation by any ligands containing oxygen as the ligating atom promotes Fe^{2+} oxidation due to the potential increase in frontier molecular orbital electron density. The latter increases Fe^{2+} basicity and,consequently, Fe^{2+} as a stronger electron donor. Similar conclusions were reached by Hood.[70] Based on the above, the surface-adsorbed –Fe(H$_2$O)$_4$(OH)$_2^+$ (Reaction 41) forms a persulfido bridge, and pyrite oxidation proceeds according to Reactions 27 through 30. However, according to Reaction 38, an alternate CO$_2$ involvement in pyrite oxidation is through formation of a pyrite/surface carboxylic acid group

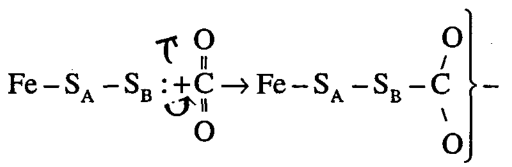

$$\mathrm{Fe-S_A-S_B:+\overset{\displaystyle O}{\underset{\displaystyle O}{\overset{\|}{\underset{\|}{C}}}} \rightarrow Fe-S_A-S_B-C}\left.\begin{matrix}\mathrm{O}\\ /\\ \\ \backslash\\ \mathrm{O}\end{matrix}\right\}- \qquad (42)$$

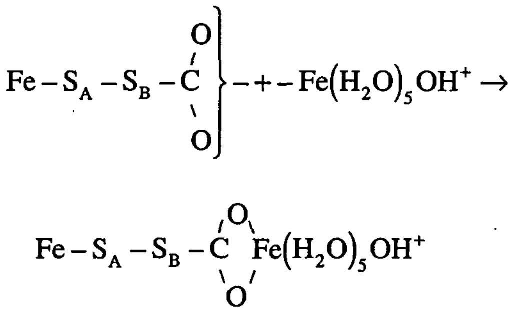

$$\mathrm{Fe-S_A-S_B-C}\left.\begin{matrix}\mathrm{O}\\ /\\ \\ \backslash\\ \mathrm{O}\end{matrix}\right\}\mathrm{-+-Fe(H_2O)_5OH^+ \rightarrow} \\ \mathrm{Fe-S_A-S_B-C}\begin{matrix}\mathrm{O}\\ \\ \mathrm{O}\end{matrix}\mathrm{Fe(H_2O)_5OH^+} \qquad (43)$$

The Fe – S$_A$ – S$_B$ – COO–Fe(H$_2$O)OH complex would promote Fe^{2+} oxidation due to the fact that the carboxylate ligand contains oxygen as the ligating atom.[97] Oxidation of Fe^{2+} to Fe^{3+}, however, is expected to produce a metastable pyrite/surface carboxylate–Fe^{3+} complex, leading to pyrite/surface decarboxylation and formation of a persulfido bridge. The latter facilitates electron transfer from S$_B$ to Fe^{3+}.

The pyrite oxidation model proposed by Moses and Herman[105] was deduced from macroscopic pyrite oxidation data, and no direct molecular evidence on most of the intermediates was presented. However, their pyrite oxidation model is consistent with frontier molecular orbital theory (see Reference 95 and references therein) and classic redox reaction theory. The proposed complementary pyrite oxidation model involving CO_2, is consistent with the model proposed by Moses and Herman[105] and the CO_3^{2-} pyrite/Fe^{2+} oxidation rate enhancement effect reported by Hood,[70] Millero and Izaguirre,[102] and Luther et al.[97]

H. Characteristics of Surface Pyrite Oxidation

Activation energies obtained for pyrite oxidation at room temperature by both ferric iron and molecular oxygen ranged from about 50 to 92 kJ /mol. These high activation energy values suggest that electron transfer reactions occurring at the pyrite surface are the rate-limiting step for pyrite oxidation.[84] Therefore, these high activation energies also suggest that the reaction mechanism for pyrite oxidation is surface controlled.

Observations made on the makeup of the pyrite surface by scanning electron microscopy have been characterized recently by using surface FT-IR techniques,[33,34,44,45,49] electrochemical techniques,[54,116] and X-ray photoelectron spectroscopy techniques (XPS).[34,112] Their results can be summarized as follows:

1. The nature of the pyrite/surface products, observed by spectroscopy, resulting from natural oxidation are dependent on the origin of pyrite (e.g., coal pyrite, mineral pyrite) and shape of pyrite (e.g., fresh fracture, polished sample, powdered mineral).
2. The mechanisms at the early stages of oxidation involve the adsorption of dissolved molecular oxygen and water on the pyrite surface and formation of various intermediates such as ferrous, ferric, sulfite and sulfate ions, sulfur, and ferric hydroxide.
3. Oxide or hydroxide films in the form of goethite, magnetite, or hematite on the oxidized pyrite surface have also been identified on various occasions.
4. Pyrite mineral surface species during oxidation by *T. ferrooxidans* are ferric and ferrous sulfate.

The presence of hydrophobic elemental sulfur or other sulfur species such as polysulfide is still open to debate. Pyrite/surface intermediates or products formed during oxidation may change the hydrophobic or hydrophilic character of the mineral surface, which may affect the oxidation process with respect to reaction rate and nature of the pyrite/surface intermediates formed.

I. Effect of Ferric Hydroxide Species on Pyrite Oxidation

Under most natural conditions (e.g., pH >4.5), Fe^{3+} exists in the natural system as ferric hydroxide or ferric oxyhydroxide solids. However, because of the ferric iron's high affinity for OH^-, ferric hydroxide solution species composed of $Fe(OH)^{2+}$, $Fe(OH)_2^+$, $Fe(OH)_3^0$ and $Fe(OH)_4^-$ are present in concentrations high enough to influence pyrite oxidation. The distribution of the ferric hydroxy species is dependent on pH.[54,63] This is demonstrated in Figure 18, which was produced employing Geochem-PC, Version 2.0. ion-association computer model.[136] Among the species shown in Figure 18, Fe(OH)^{2+} and Fe(OH)_2^+ are more interesting because these positively charged ions may be adsorbed, as a result of electrostatic interactions, by the negatively charged pyrite surface at pH values near or higher than the isoelectric point of pyrite, which is slightly greater than pH 1.[54] A pyrite/surface-Fe(OH)_n^{n-3} complex could form according to the following reaction

$$-\text{Fe}-\text{S}-\text{S}^- + \text{Fe(OH)}_n^{3-n} \rightarrow -\text{Fe}-\text{S}-\text{S}-\text{Fe(OH)}_n^{3-n} \qquad (44)$$

Representative relationships between pH and adsorbed Fe(OH)^{2+} and Fe(OH)_2^+ are shown in Figure 19. These iron species, Fe(OH)^{2+} and Fe(OH)_2^+, are primarily adsorbed at low pH (<3) and circumneutral pH, respectively. It is unknown,

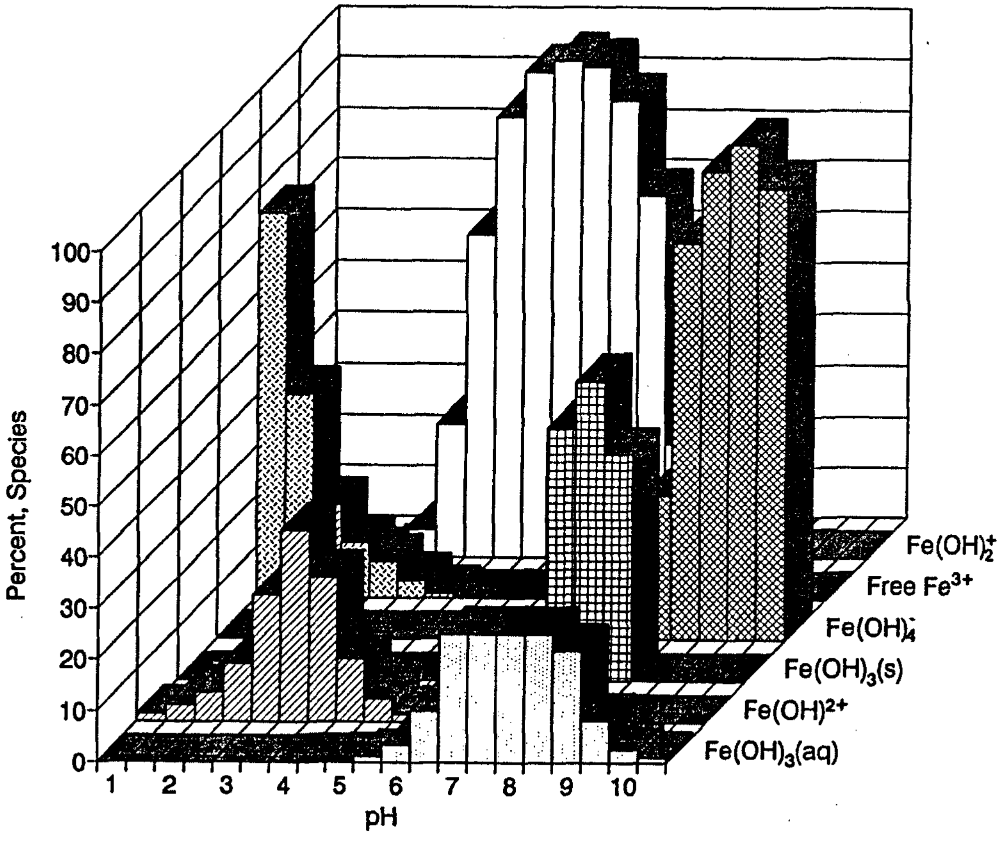

FIGURE 18. Percent of ferric-hydroxy species as a function of pH.

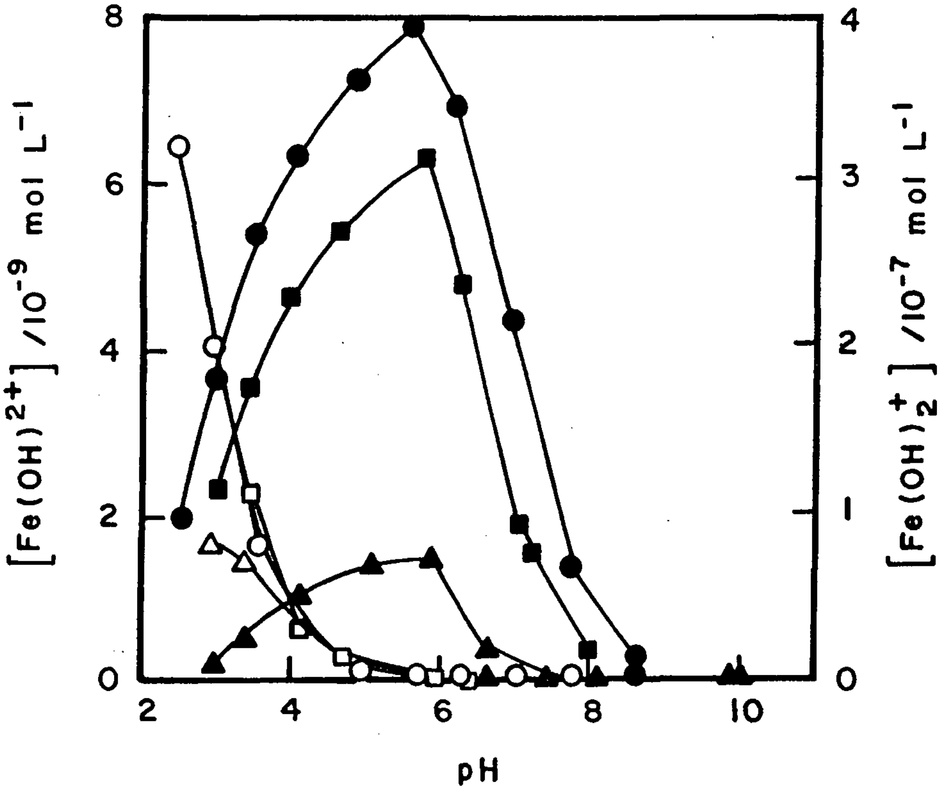

FIGURE 19. Concentration of $Fe(OH)^{2+}$ and $Fe(OH)_2^+$ adsorbed on pyrite as a function of pH. Open symbols represent $Fe(OH)^{2+}$; closed symbols represent $Fe(OH)_2^+$; triangles denote 0.5 h in air; squares denote 2 h in air; circles denote 19 h in air. (After Fornasiero, D., Eijt, V., and Ralston, J., *Colloids Surf.*, 62, 63, 1992.)

however, to what degree the rate of pyrite oxidation is related to the concentration of these two iron-hydroxy species on the surface of pyrite. It is important to note that the formation of iron-hydroxy species in the solution phase as a function of pH (Figure 18) appears to be related to the formation of iron-hydroxy species on the pyrite surface (Figure 19). The presence of OH^- as $Fe(III)(OH)_n^{n-3}$ on the pyrite surface is most likely involved in the electron transfer process between the disulfide and Fe(III).[19,20] Increase of abiotic pyrite oxidation rate as a function of pH may in fact be related to the increase in the availability of surface OH^-.

J. Measurement of Reaction Progress Variables

Several reaction progress variables (RPV) can be chosen by investigators to determine the rate of pyrite oxidation. Each selected RPV has its own inherent strengths and weaknesses, which often change depending on the information sought and the oxidation conditions used. Oxidation reaction rates based on measurement of total iron in solution have been shown to be an accurate indicator of reaction progress in low-pH studies,[98] but their use in neutral to higher pH is precluded due to the low solubility of $Fe(OH)_3$ under these conditions.

Nicholson et al.[111,112] chose sulfate as the rate-indicating variable and assumed under their experimental conditions that there was complete oxidation of intermediates to sulfate.[106] On the other hand, Hood[70] used experimental conditions similar to those of Nicholson et al.[12] and found that sulfur-containing species, other than sulfate, constituted a significant proportion of the total sulfur. Furthermore, the proportion of the sulfur present as sulfate was found to vary with certain experimental parameters such as pH, O_2, and Fe^{3+}.[106]

Measurement of the pyrite oxidation rate based on changes in the oxidation potential of the iron couple is operative in acidic conditions, especially pH <2, in which ferric iron hydrolysis and oxidation of ferrous iron are negligible and the activity of the free ferric ion is high compared with the activity of ferric complexes.[157]

Measurement of the change in total weight or volume of pyrite is considered inappropriate RPV because of very low sensitivity at a low percentage of reaction as well as difficulties encountered due to solid oxidation product formation and surface retention, such as iron oxide or ferrous sulfate.[49,112]

It has generally been concluded that measurement of pyrite oxidation has a degree of uncertainty. The level of uncertainty decreases as the system variables are better understood.

IV. ACID MINE DRAINAGE

Acid mine drainage (AMD) results primarily from the oxidation of pyrite and other iron sulfides in coal waste, ore tailings, and overburden, and is a severe environmental pollution problem associated with coal and other sulfide-containing ore-mining operations. AMD is extremely acidic (as low as pH 2) enriched with soluble iron, manganese, aluminum, sulfate, and at times heavy metals such as Pb, Hg, Cd, etc. Oxidation of pyrite mediated by Fe^{3+} and O_2 has been accepted as the major cause for production of AMD However, other mechanisms, including pyrite oxidation mediated by Mn- and Fe-oxides, weathering of minerals, and ferrolysis, may contribute to AMD production.

A. Mn- and Fe-Oxide Involvement in Acid Mine Production

The ferric iron, as mentioned above, is the major oxidant of pyrite regardless of pH, which implies that any reactions producing Fe^{3+} will indirectly result in the oxidation of pyrite. Asghar and Kaehiron[3] observed that Fe^{2+} can be oxidized to Fe^{3+} in the presence of manganese oxides at pH ≤5.5, as shown below

$$MnO_2 + 4H^+ + 2Fe^{2+} = Mn^{2+} + 2H_2O + 2Fe^{3+} \tag{45}$$

Asghar and Kaehiron[3] also reported that 95% of 100 ppm of ferrous sulfate was oxidized to ferric within a day when added to a soil sample of pH 4.4 and manganese content of 3.04%. Luther et al.[97] indicated that dissolution of ferric iron minerals (e.g., goethite FeOOH) permit direct formation of aqueous Fe^{3+} complexes as follows:

$$FeOOH + 3H^+ \rightarrow Fe^{3+} + 2H_2O \tag{46}$$

$$\begin{aligned} &FeOOH + C_6H_4(OH)_2 \rightarrow \\ &\quad \{Fe^{3+}[C_6H_4(OH)_2]\}^+ + H_2O \end{aligned} \tag{47}$$

or

$$\begin{aligned} &FeOOH + 3H^+ + \text{Ligand} \rightarrow \\ &\quad Fe(III) - \text{Ligand} + OH^- \end{aligned} \tag{48}$$

Reaction 46 is well known and is the basis of many analytical methods for some minerals containing Fe(III). Reaction 47 represents the dissolution of Fe(III) minerals by siderophores (ligand), of which catechol ($C_6H_4(OH)_2$) is a common component.[68] The ligands in Reaction 48 are weak-field organic acids produced by plant and bacteria and generally contain oxygen in the form of hydroxyl or carboxyl functional groups.[68] Some mine waste and coal residue are known to contain large quantities of Mn and Fe oxides.[8,85] Ferric iron produced through the above reactions may oxidize pyrite, as previously detailed.[97]

B. Ferrolysis and Acid Mine Drainage Production

The process of ferrolysis can produce acid drainage in geologic material where $Fe(OH)_3$ and $CaSO_4 \cdot 2H_2O$ are known to form on pyrite oxidation and product neutralization by limestone. Ferric trihydroxide ($Fe(OH)_3$) is for the most part water insoluble at pH values greater than 3.5. Under reducing conditions, $Fe(OH)_3$ transforms to $Fe(OH)_2$,[141,142] which is quite soluble up to pH 8.[87] On the other hand, in the same pH range, $CaSO_4 \cdot 2H_2O$ is quite insoluble (15 mmol/l).[48,50] Enrichment of pore water with Fe^{2+} and depletion of Ca^{2+} (either through leaching or chemical equilibria considerations of $CaSO_4 \cdot 2H_2O$) promotes displacement of Ca^{2+} from the exchange sites of mine waste by replacement with Fe^{2+}. After returning to strong oxidation conditions, the Fe^{2+} adsorbed on the surface of charged minerals undergoes oxidation and hydrolysis, releasing relatively large quantities of acid. Reactions 49 and 50 demonstrate the process of ferrolysis.

$$\text{Surface} - \text{Ca} + \text{Fe}^{2+} \rightarrow \text{Surface} - \text{Fe(II)} + \text{Ca}^{2+} \tag{49}$$

$$\text{Surface} - \text{Fe(II)} + \text{O}_2 \rightarrow \text{Surface} - \text{Fe(III)} + \text{H}^+ \tag{50}$$

Ferrolysis is a well-known phenomenon in iron-rich soil/environments under high rainfall/leaching and alternating oxidation/reduction conditions.

V. PREVENTION TECHNOLOGIES OF ACID MINE DRAINAGE

Federal water quality standards in the U.S. require that mine discharges have a pH between 6 and 9, and total iron and manganese concentrations equal to or less than 3.0, and 2.0 mg/l, respectively. At many active and inactive mine sites, drainage does not meet these standards and needs to be treated before it is discharged. In the U.S., the mining industry spends over $1 million per day to treat AMD.

The U.S. Bureau of Mines estimated that abandoned coal and metal mines and the associated piles of mine waste adversely affect over 12,000 mi of river and streams, and over 180,000 acres of lakes and reservoirs in the U.S.[77] Wildeman[158] pointed out that handling the environmental aspects of a coal mining operation can be just as costly as the actual coal extraction, and abatement of already present AMD is far more troublesome than planning to avoid the problem.

Conventional and current technologies used to avoid the production of AMD at the source and to abate AMD are reviewed below. These include conventional methods of inundating and neutralizing pyritic material and current methods employing wetlands, limestone, and phosphate.

A. Inundation of Pyritic Material

Inundation of pyritic materials is a conventional method generally used in curtailing AMD. Oxygen diffusion to pyritic wastes is greatly reduced after inundation because the diffusion coefficient of O_2 through the covering water table is only 1/10,000 of that through the waste atmosphere.[115] Thus, the rate of O_2-consuming reactions becomes low and rate limiting, and bacterial oxidation of pyrite becomes slow or nil. Kleinmann and Crerar[80] confirmed that there was no significant growth of *T. ferrooxidans* in water-saturated environments. However, complete inhibition of pyrite oxidation by flooding may never be possible because of the availability of Fe^{3+} as an alternate oxidant. A field study by Foreman,[53] a laboratory column leaching study by Watzlaf,[154] and an O_2-free incubation by Pionke et al.[118] have shown that when pyritic waste was flooded, there was usually a significant, albeit incomplete, reduction of acidity.

Underwater disposal of pyritic materials has been used by the metal mining industries with some success.[123] Bell[10] summarized the opinion of many people concerned with metal mine disposal as follows: "At the current time, the only practical and proven long-term approach to controlling the formation of acid in sulfide tailings is to limit the availability of oxygen as a reactant by maintaining the waste in a saturated or submerged condition." However, concerns with underwater disposal include the potential presence of dissolved O_2 and Fe^{3+}, two pyrite oxidants, as well as being able to maintain complete and continuous water saturation. Biotic oxidation of pyrite is not limited until pore gas oxygen is reduced to less than 1%.[21,64] One may argue that based on current reclamation practices, this low level of O_2 will be hard to attain. Fluctuations in the level of the water table usually cause incomplete inundation and move the active oxidation zone to a higher elevation in the mine, promoting acid formation.

Because of the increasing recognition of the importance of wetland formation and retention, and the large amount of pyritic waste requiring disposal, burying pyritic materials beneath wetlands has been suggested. Like inundation, wetlands provide a cover of water that isolates pyritic waste from the atmosphere and prevents oxidation and acid formation. Nevertheless data are needed to evaluate the role of O_2 released from the roots of aquatic plants, growing in the wetlands, in pyrite oxidation. Zhang et al.[159] employing microelectrodes, measured the rhizosphere pH and redox potential (Eh) of a pyrite soil in a wetland with cattail (*Typha latifolia* L.). They found that (1) the rhizosphere pH was one unit lower than the bulk soil pH, (2) the oxidation potential and sulfate concentration of the rhizosphere were higher than in bulk soil, and (3). iron oxide and oxyhydroxide were on the root surfaces and on the soil immediately adjacent to root surfaces. They concluded from these observations that cattail roots can significantly oxidize pyrite present in the rhizosphere. They also suggested that time scale and root density may be an important consideration for predicting the amount of oxidized pyrite when buried beneath a cattail wetland.

B. Neutralization by Alkaline Materials

Alkaline chemicals, such as limestone or sodium hydroxide, are usually applied or pumped into active mines where AMD is a problem. Alkalinity derived from limestone acts as pH buffer and AMD neutralizer; it also hydrolyzes most heavy metals, thus precipitating them as metal hydroxides. If sufficient alkaline material is added and the nature of this alkaline material is such that it is able to raise the pH up to 9, most of the metals will be hydrolyzed and precipitated. Metals such as iron and manganese must be oxidized before being precipitated as stable compounds, which is why aeration and neutralization are combined in treating AMD in active mine sites. Other materials, such as alkaline fly ash and topsoil or their mixtures with lime, have been found to significantly reduce drainage iron concentration as well as manganese and sulfate.[75]

Limestone is readily available in most coal mining areas and has considerable cost advantage over other alkaline materials. However, limestone is not as effective in controlling AMD as one might expect because of its limited solubility and its tendency to armor with ferric hydroxide precipitates.[156] When mine waters enriched with iron contact limestone in an oxidizing environment, the limestone is coated rapidly with ferric hydroxide precipitates. The rate of dissolution of the coated limestone is inhibited, and production of alkalinity is significantly diminished.

When AMD comes in contact with limestone in an anoxic environment, limestone dissolution and subsequent production of alkalinity can proceed without inhibitory armoring. The idea of generating alkalinity in anoxic limestone drains (ALD) is given close attention for its effectiveness of treating AMD.[16,109,110,149,155] An anoxic limestone drain can be constructed as follows. An excavation is made to intercept the AMD in surface mine waste or spoil. The excavation is filled with limestone and then covered by plastic and clay to inhibit oxygen penetration and loss of carbon dioxide gas. Under these conditions, limestone will be dissolved at a higher rate due to lowering pH caused by the higher partial pressure of carbon dioxide ($^{P}CO_2$). Furthermore, iron armoring of limestone will be eliminated due to inhibition of iron oxidation. The water discharged from ALD contains a significant concentration of HCO_3^- and relatively high concentrations of iron and manganese, if present. This water is then aerated, and metal oxidation, hydrolysis, and precipitation occur in a strongly buffered alkaline solution of a settling pond or constructed wetland. The scheme of the entire passive ALD treatment system is shown in Figure 20. Nairn et al.[110] tested an anoxic limestone drain in a surface mine site and found out that the water discharged exhibited circumneutral pH (pH 6 to 8) and considerable metal removal occurred in the pond and constructed wetland following the drain.

A more recent approach in controlling AMD production was the use of an alkaline recharge (e.g., NaOH, $CaCO_3$).[30,83] Neutralizers such as sodium hydroxide, because of their high solubility, can be easily moved with percolating water deep in the strata to sites where acid drainage is produced. Thus, no physical mixing of the strata with the ameliorator is required. However, effectiveness lasts only as long as someone supplies neutralizers. This is extremely costly and not very practical.

C. Wetland Treatment System

Over the last decade, wetlands have being constructed to treat AMD. The wetland processes previously identified as having the potential for removing metals from AMD include adsorption of metals by ferric oxyhydroxides, plant and algae uptake of metals, complexation of metals by organic materials, and precipitation of metals into oxides, oxyhydroxides, and sulfides. From the above processes, only precipitation as either oxides or sulfides have long-term metal removal

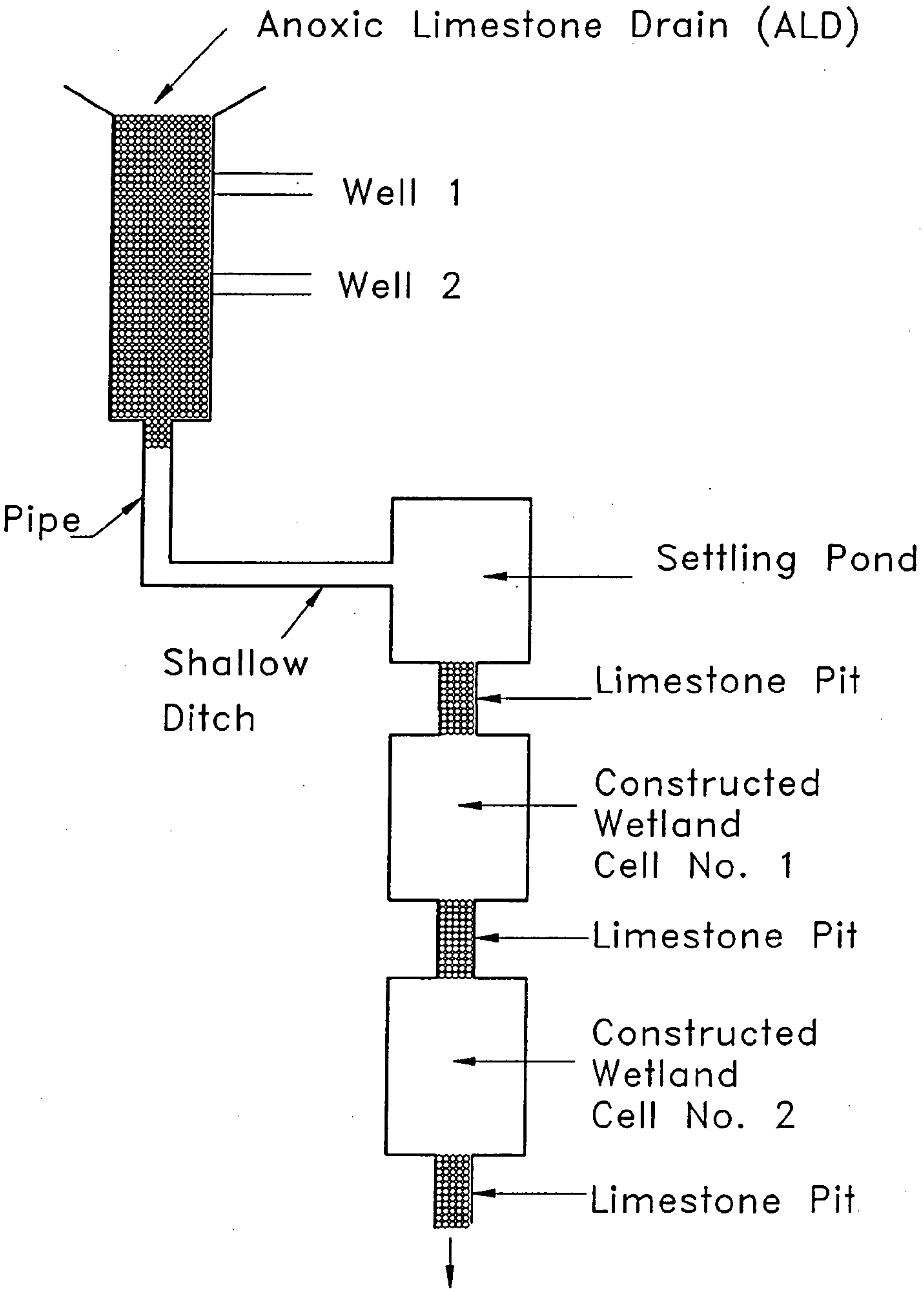

FIGURE 20. Schematic of the entire passive anoxic limestone drain (ALD) treatment system.

potential. The rest of the processes are considered to be insignificant or to have finite capacity.

Wetland may be a poor environment for the formation of metal oxides and oxyhydroxides because of the typically low redox potential (Eh) associated with wetland and wetland sediments. Studies are now focused on optimizing the activity of sulfate-reducing bacteria that thrive in the anaerobic zone of wetland. These sulfate-reducing bacteria consume acidity, and most of the hydrogen sulfide they produce reacts with heavy metals to yield insoluble precipitates. Results from column and reactor studies simulating reducing conditions indicated that trace metals such as Co, Cu, Cd, Ni, Pb, and Zn can be removed as sulfides[38,65,138] It must be emphasized that in order for significant SO_4 reduction to occur, the high-sulfate AMD must flow through the anaerobic portion of the wetland. However, according to Wildeman,[158] the typical natural wetland and most constructed wetlands may not have sufficient permeability to fully take advantage of this process.

D. Inhibition of Iron-Oxidizing Bacteria

Anionic surfactants (common cleaning detergents), organic acids and food preservatives have been used as pyrite oxidation inhibitors by controlling bacterial growth,[36,41,79] In the presence of such compounds, bacteria allow hydrogen ions in the acidic environment to move freely into or through cell membranes, causing their deterioration.

U.S. Bureau of Mines researchers,[77] showed that anionic surfactants decrease the activity of bacteria and thereby retard pyrite oxidation. They also reported that anionic surfactants were most applicable to coal refuse piles and isolated zones of fresh pyrite material, reducing acid production by 60 to 95%. The surfactants sprayed or applied on the surface mine are now commercially available. However, wide use of anionic surfactants is limited for two specific reasons. (1) Anionic surfactants are very soluble and move with water, thus repeated treatments are required to prevent bacteria repopulation. (2) Anionic surfactants may also be adsorbed on the surfaces of minerals and may not reach the pyrite-bacteria interface.[41,126]

E. Inhibition of Pyrite Oxidation by Phosphate

The potential of Fe^{3+} to act as a pyrite oxidant can be reduced by the addition of phosphate. Phosphate can precipitate Fe^{3+} in an insoluble form as $FePO_4$ or $FePO_4$ $2H_2O$ (strengite).[7,70,73] Spotts and Dollhopf[137] evaluated two sources of apatite and two phosphate byproducts applied at a concentration of 30 g/kg by weight to pyritic mine overburden. Their results indicated that the materials are effective for the control of pyrite oxidation. However, Huang and Evangelou[72] carried out a series of experiments to demonstrate that phosphate applications indeed limit pyrite oxidation. The results of these studies indicated that this inhibition is only temporary because of iron armoring.[51,72]

Recently, Huang and Evangelou[73] and Evangelou,[45] using small leaching columns, have developed two new microencapsulation (coating) methodologies for preventing pyrite oxidation and acid production in coal pyritic waste. The first coating methodology involves leaching coal waste with a solution composed of low but critical concentrations of H_2O_2, KH_2PO_4, and a pH buffer. During the leaching process, H_2O_2 oxidizes pyrite and produces Fe^{3+} so that iron phosphate precipitates as a coating on pyrite surfaces. The purpose of pH buffer in the coating solution is to eliminate the inhibitory effect of the protons, produced during pyrite oxidation, on the precipitation of iron phosphate. The coating process is shown schematically in Figure 21.

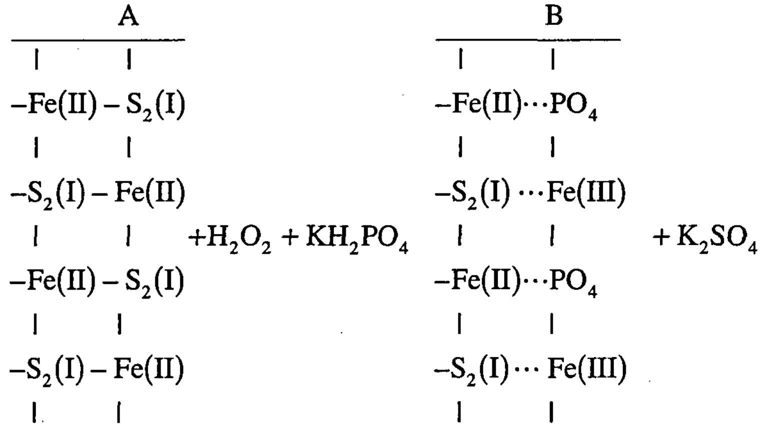

FIGURE 21. Schematic of H_2O_2-induced oxidation proof phosphate surface coating.

The dotted lines in B signify physical bonding between pyrite and $FePO_4$. When iron (Fe^{3+}) reacts with PO_4^{3-} it forms a highly acid resistant ferric phosphate ($FePO_4$) coating, which inhibits the oxidation of pyrite shown in Figure 22, from which the big difference in the release of SO_4 from coated and uncoated pyrite in coal waste material strongly suggests that surface pyrite coating, if it can be applied successfully at the field level, could be effective in controlling the oxidation of pyrite. The ferric phosphate coating alters the microscopic surface morphology of the pyrite grains (Figure 23A, B).

A second coating methodology involves leaching pyritic waste with a solution composed of low but critical concentrations of H_2O_2 and a pH buffer. During the leaching process, H_2O_2 oxidizes pyrite and produces an iron oxide coating on the surface of pyrite (Figure 23C). The purpose of a pH buffer in this case is to buffer the solution during coating formation at a pH between 5 and 7, where iron oxide formation is promoted.

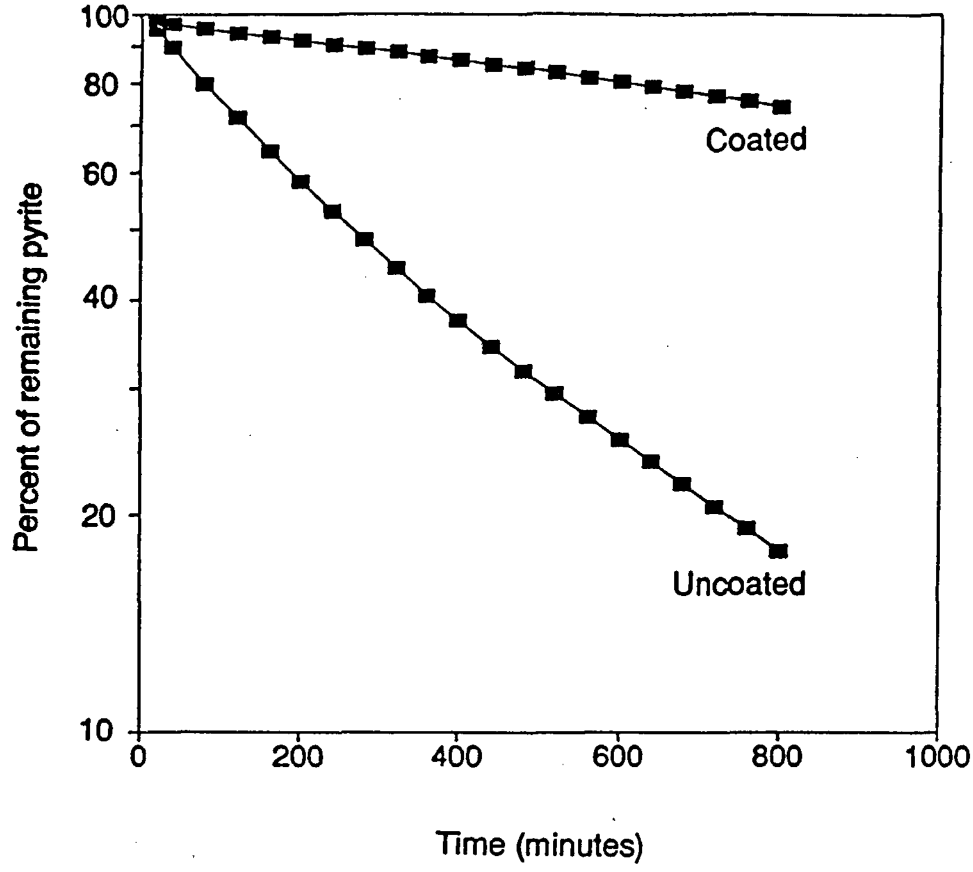

FIGURE 22. Sulfate release from 0.5 g pyritic coal waste microcolumns with and without ferric phosphate coatings using H_2O_2. (From Evangelou, V. P., *J. Environ. Qual.*, submitted. With permission.)

Successful application of such coating methodologies in the field could mean a long-term solution (perhaps even a permanent solution) to certain types of AMD problems. These coating methodologies are expected to be highly cost effective because they involve readily available materials and only cover the surface of the pyrite particles. Furthermore, the coating solution could be applied to any permeable coal mine waste; thus, little or no physical disturbance of coal mine waste during treatment would be necessary.

It is important to note that the technology of coating pyrite as described above is not to be confused with the field application of rock phosphate.[52] Rock phosphate complexes dissolved iron (Fe(II)) and thus reduces the potential of Fe(III) production, reducing the potential for pyrite oxidation as well.[141] Rock phosphate does not

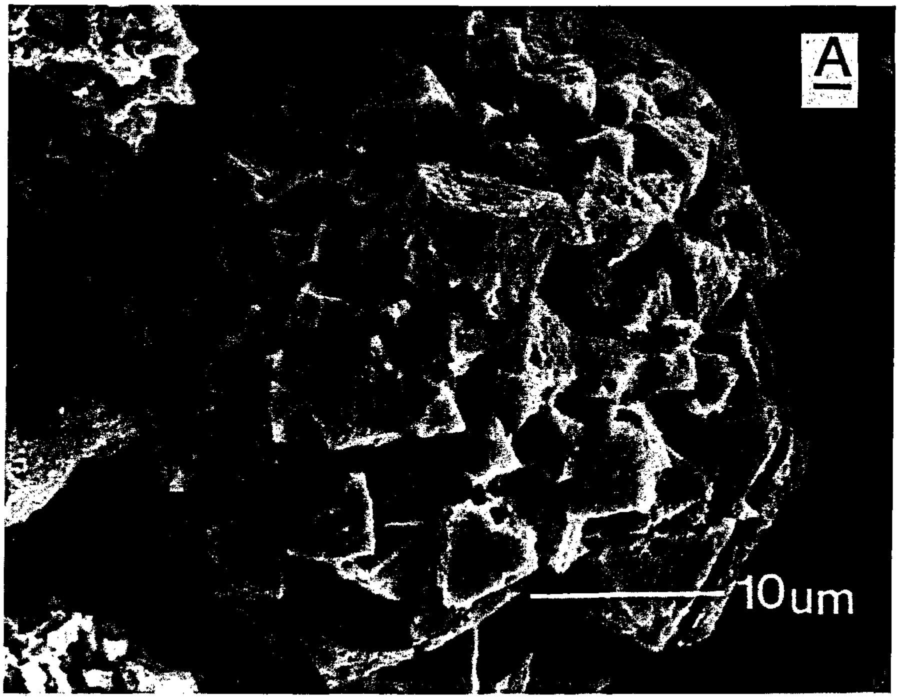

A

FIGURE 23. Scanning electron microscope photos showing the morphology of the framboidal pyrite particles. (A) Without coatings; (B) $FePO_4$ coatings; (C) with iron oxide coatings. (From Evangelou, V. P., *J. Environ. Qual.*, submitted. With permission.)

coat pyrite; rather, it complexes released Fe(II) from the oxidizing pyrite.[51] Instead, a rock phosphate surface coating with Fe(II) forms, reducing rock phosphate dissolution. Therefore, the effectiveness of rock phosphate in controlling pyrite oxidation is short lived.

F. Prediction of Acid Drainage Potential

There are several methods or approaches for predicting the potential of pyritic geologic material to produce AMD. These approaches include (1) determination of potential acidity in pyrite overburden, (2) acid-base accounting, (3) simulated weathering, and (4) computer simulation modeling. A brief discussion of each of these approaches appears below.

1. Determination of Potential Acidity

It is often necessary to quantify the acid-producing potential of geologic strata before surface mining or before land reclamation is started. To prevent excessive

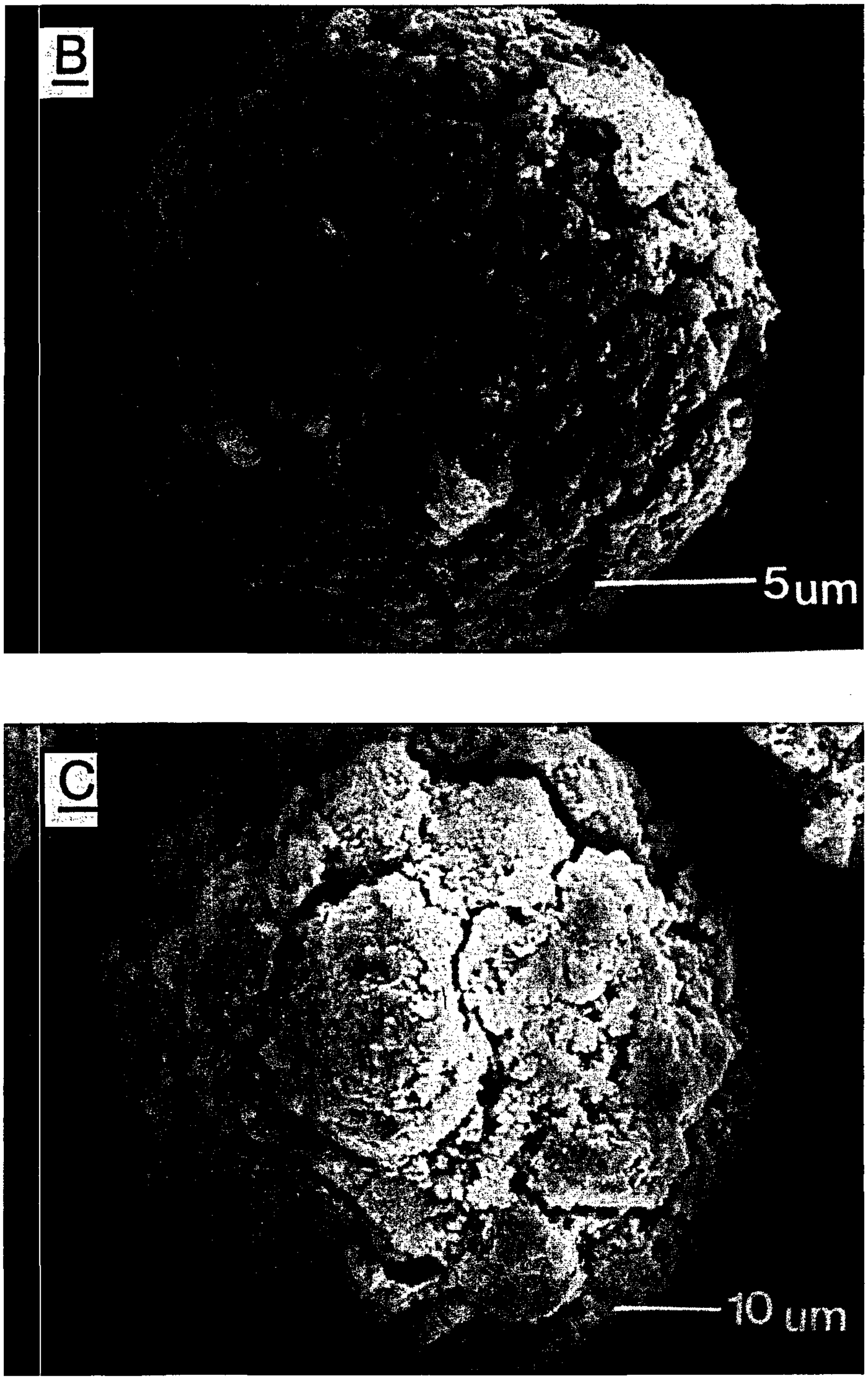

FIGURE 23.B,C

acidity problems that could occur after leveling of the disturbed geologic strata, a rapid, accurate, and reproducible potential acidity method is required. Several methods for determining potential acidity have been proposed.[4,23,107,134] Each of these methods measures either sulfur or iron associated with pyrite and therefore provides an indirect estimate of the potential acidity. A direct determination of acid-producing potential is the rapid pyrite oxidation technique utilizing 30% H_2O_2. The actual acid produced during pyrite oxidation by H_2O_2 is termed potential acidity.[114,133] The technique determines the amount of acid produced during complete oxidation of the Fe^{2+} and S_2^{2-} of pyrite as follows:

$$\begin{aligned} &FeS_2 + 7.5H_2O_2 \rightarrow \\ &\quad Fe(OH)_3(s) + 2H_2SO_4 + 4H_2O \end{aligned} \tag{51}$$

Reaction 51 demonstrates that complete pyrite oxidation liberates 2 mol of H_2SO_4 for every mole of FeS_2 oxidized. Two other moles of H^+ are produced during Fe^{3+} hydrolysis and precipitation as $Fe(OH)_3$.

2. Acid-Base Accounting

Acid-base accounting is the most widely used method for characterizing overburden geochemistry because it is simple, relatively inexpensive, and reliable. The three fundamental measurements comprising an acid-base accounting are pH, percent of total sulfur or pyritic sulfur, and neutralization potential. The purpose of acid-base accounting on a geologic sample is to identify the acid-producing potential due to pyrite and the neutralization-producing potential due to alkaline material such as rock carbonates. The difference between the two potentials indicates if there is enough base present to neutralize all acid that is to be produced from the oxidation of pyrite.[132]

Caruccio and Geidel[26] criticized the technique of acid-base accounting because it does not consider differences between the rate of pyrite oxidation and the rate of carbonate dissolution. Furthermore, the technique considers that all pyrite present in the sample is oxidizable under natural oxidizing conditions. Acid-base accounting has been applied with some success to mine planning in the East, Midwest, Western coal fields of the U.S., and is used in overburden analysis in Canada, Australia, and Russia.[130]

3. Simulated Weathering Technique

The basic idea of simulated weathering is to leach natural overburden or spoil in laboratory-scale experiments with the idea that results are applicable to the field.

The effluent is collected and analyzed for pH, acidity, sulfate, iron, etc. The results of these analyses are used to evaluate AMD formation potential.

Probably the best known simulated weathering technique is attributed to Caruccio and Geidel,[26] who determined the acid-producing potential by titrating the leachates produced from oxidation of geological material in the presence of humid air, followed by periodic distilled water washing. Sturey et al.[143] developed a leaching procedure in which various rock types are mixed and treated to simulate the potential sequence of materials placement in a backfill. Leaching with acid water (inoculated with *Thiobacillus* bacteria) allows for accelerated pyrite oxidation and provides a small-scale model to predict drainage quality.

One of the advantages of simulated weathering is that it considers the relative weathering rates of pyrite and carbonate materials. It is, however, still very difficult to say to what degree the technique resembles a mine waste profile where the roles of factors such as oxygen diffusion, water infiltration, bacteria effectiveness, and salt and clay mineral influences on pyrite oxidation are unknown.

4. Computer Simulation Models

Computer simulation models are perhaps the best way to predict AMD formation potential because such models can incorporate a maximum number of interactive variables affecting pyrite oxidation.[17,18,76,121,124,125] These models are based somewhat on theory and are derived from column leaching and field observations. Model validation is carried out by comparing model predictions with field measurements in some range of conditions. By reviewing these models, it appears that the model by Jaynes et al.[76] and that by Bronswijk and Groenenberg[17] are currently the best mechanistic/functional approaches to describe the oxidation process as controlled by inorganic physical and biophysical chemistry.

Jaynes's model considers that pyrite oxidation is carried out directly by O_2 and Fe^{3+}. The concentration of O_2 is predicted by diffusion, whereas that of Fe^{3+} is assumed to be controlled by the solubility product of $Fe(OH)_3$ and the oxidation potential. Jaynes's model also describes some processes at the microscopic/molecular level. Such processes include adsorption of O_2 and Fe^{3+}, their reduction through electron transfer, and generation of reaction products and product detachment from the surface of oxidizing pyrite. However, the biggest weakness of Jaynes's model is the simplicity with which it treats solute transport relative to the actual complexity of the process, and its failure to consider the complex molecular surface chemical processes involved in solution and the pyrite surface during oxidation. The computer simulation model by Bronswijk and Groenenberg[17] is more advanced in predicting pyrite oxidation in alkaline environments. This model assumes that in an alkaline environment, O_2 diffusion is the rate-limiting step of pyrite oxidation and that O_2 is the only pyrite oxidant. The model is more sophisticated than Jaynes's model with respect to surface exchange reactions, dissolution/

precipitation, and solute transport reactions. The role of Fe^{3+} as an oxidant was not assigned in this model.

The model by Jaynes et al.[76] and Bronswijk and Groenenberg[17] represent the state of the art in AMD modeling. However, for the most part, these models do not represent state-of-the-art knowledge available on pyrite oxidation. Clearly, the potential for puting together improved computer models for predicting AMD formation is high.

VI. SUMMARY

AMD is a severe environmental pollution problem associated with coal and other sulfide-containing ore mining operations and results mainly from the oxidation of pyrite. AMD is extremely acidic (pH as low as 2) and enriched with iron, aluminum, sulfate, and heavy metals such as Pb, Hg, Cd, etc. It is estimated that each year in the U.S., wet cleaning of coal alone leaves behind aqueous slurries of refuse containing at least 10 million tons of pyrite.[14] The need to prevent AMD formation has thus triggered numerous investigations into the mechanisms of pyrite oxidation.[19,20,70,105,106,111,112,129]

Pyrite in mining waste is initially oxidized by atmospheric O_2, producing H^+, SO_4^{2-}, and Fe^{2+}

$$FeS_2 + 7/2O_2 + H_2O \rightarrow Fe^{2+} + 2SO_4^{2-} + 2H^+ \tag{52}$$

The Fe^{2+} produced can be further oxidized by O_2 into Fe^{3+}, which in turn hydrolyzes into iron hydroxide and releases additional amounts of acid into the environment.[113]

$$Fe^{2+} + 1/4O_2 + H^+ \rightarrow Fe^{3+} + 1/2H_2O \tag{53}$$

and

$$Fe^{3+} + 3H_2O \rightarrow Fe(OH)_3 + 3H^+ \tag{54}$$

Most iron released during the initial stages of pyrite oxidation ends up as iron hydroxide due to the relatively high pH on pyrite surfaces.[54,74] However, when pH in the vicinity of the pyrite surfaces drops below 3.5 (due to acid production), the activity of free Fe^{3+} in solution increases and oxidation of pyrite by Fe^{3+} becomes the main mechanism for acid production. Singer and Stumm[129] reported that Fe^{3+} can oxidize pyrite at a much higher rate than O_2.

The role of Fe^{3+} in the oxidation of pyrite is demonstrated below:

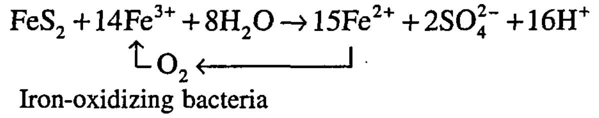

$$\begin{tikzcd}[column sep=small] FeS_2 + & 14Fe^{3+} & + 8H_2O \rightarrow & 15Fe^{2+} + 2SO_4^{2-} + 16H^+ \arrow[dll] \\ & O_2 \arrow[u] & & \end{tikzcd} \tag{55}$$

Iron-oxidizing bacteria

At low pH, an acidophilic, chemoautotrophic, iron-oxidizing bacterium, *T. ferrooxidans*, catalyzes and accelerates the oxidation of Fe^{2+} by a factor larger than 10^6.[129] Thus, the processes of reduction of Fe^{3+} to Fe^{2+} by atmospheric O_2, catalyzed by *T. ferrooxidans*, constitute an effective continuous pyrite oxidation cycle. For this reason, *T. ferrooxidans* is considered to be primarily responsible for the rapid oxidation of pyrite in mine waste at low pH.[113] Based on the above, pyrite oxidation can be significantly reduced by complexing/precipitating Fe^{3+}, inhibiting Fe^{3+} production, and depriving the system of oxygen (O_2).[41,76,125]

It is commonly believed that pyrite oxidation can be controlled by adding alkaline material to pyrite, a widely used field practice. This is due to the fact that at high pH *T. ferrooxidans* activity diminishes and Fe^{3+} becomes insoluble (see Reference 76 and references therein). However, recent findings[105] showed that the nonmicrobial pyrite oxidation rate increased as pH increased. At high pH, nonmicrobial pyrite oxidation appeared to be carried out by a surface-catalyzed mechanism involving Fe^{2+}, O_2, and Fe^{3+}; the latter's low water solubility at high pH (>3.5) did not appear to be a rate-limiting factor. Data from Brown and Jurinak[19] and Hood[70] also supported these findings. According to Luther[95] and references therein, pyrite/surface-exposed disulfide provides a slightly negatively charged pyrite surface due to an unshared pair of electrons that attract ions willing to share them (e.g., $Fe^{2+)}$. Moses and Herman[105] concluded that because of this unshared pair of electrons, the pyrite/surface behaved as a soft base (see Reference 135 and references therein) showing higher preference for Fe^{2+} than for Fe^{3+} because the former is a relatively softer Lewis acid. However, pyrite/surface-adsorbed Fe^{2+} in the presence of O_2 rapidly oxidizes to Fe^{3+}, depending on surface pH. Fornasiero et al.[54] demonstrated the formation of $Fe(OH)_n^{3-n}$ complexes on the surface of pyrite after exposure to O_2. Hood[70] concluded that the cause of the increase in the rate of pyrite oxidation under alkaline conditions was the formation of a pyrite/surface-CO_3 complex that facilitated electron transfer and rapid turnover of Fe(II) to Fe(III)[102] However, Hood[70] failed to provide any direct molecular evidence for this pyrite/surface-CO_3 complex.

An accepted mechanism explaining the enhancement of nonmicrobial pyrite oxidation in high pH environments is OH^- involvement in an inner-sphere electron transfer process.[20,95] In this process, an OH^- and an electron are exchanged simultaneously between pyrite/surface-Fe(III)$(OH)_n^{3-n}$ and pyrite/surface disulfide. Data in the literature also show that CO_3^{2-} promotes nonmicrobial pyrite oxidation.[70] Evangelou and Huang[49] using FT-IR spectroscopy demonstrated that pyrite exposed to humidified CO_2 plus O_2 formed pyrite/surface-CO_x complexes. Two potential mechanisms were proposed to account for these complexes. One mechanism involved formation of a weak pyrite/surface-Fe(II)–CO_3 complex, whereas the second mechanism involved formation of a pyrite/surface-carboxylic group complex (–Fe(II)–S–S–COO^-). Based on the above results, Evangelou and Huang[49] postulated that CO_2 (owing to its potential to react with surface -OH) tended to form weak pyrite/surface-Fe(II)–CO_3 complexes that would promote nonmicrobial pyrite oxidation by accelerating Fe(II) oxidation. The latter has been validated in previously published studies employing ferrous-carbonate solution systems[102] On the other hand, formation of $-Fe-S-S-COO^-$ could be implicated in promoting nonmicrobial pyrite oxidation by facilitating an inner-sphere electron transfer from the pyrite/surface disulfide to the pyrite/surface-Fe(III)$(OH)_n^{n-3}$ complex.[44,45]

Currently, acid metallic drainages produced by Fe-sulfide oxidation are controlled by several approaches: (1) application of limestone/rock phosphate or sewage sludge, (2) application of bactericides, (3) creation of fully anoxic environments by using clay liners, plastic liners, asphalt, etc., and (4) establishment of wetlands. The first two acid drainage remediation technologies only slow down the production of acidic drainages, but do not stop it, and have a short life span due to the coating potential (armoring) of limestone/rock phosphate by iron oxides [89,139,140] This limestone/rock phosphate-coating problem is commonly observed in the field, and we have carried out extensive investigations in our laboratory on the factors causing it.[51] All these materials have one major limitation. They are difficult to apply in actual sites where AMD is produced, and due to their low solubility, they require physical mixing with the sulfide-rich strata.

Application of bactericides has a suppressing effect on the activity of *T. ferrooxidans*. Kleinmann[81] was one of the first to introduce bactericidal control on acid drainage. Slow-release pellets of such bactericides are currently available in the market.[119] The major disadvantages of this approach are (1) AMD is suppressed for relatively short periods, and chemical oxidation of pyrite by O_2 is not inhibited by bactericides; (2) for acid drainage produced at lower depths of a geologic stratum, mixing of the pellets with the material is cost prohibitive; and (3) bactericides do not have much of an effect on acid metallic drainages produced prior to treatment, and the strata continue to discharge "acid effluents" during water flows.

A more recent approach in controlling AMD production was the use of alkaline recharge (e.g., NaOH). However, the effectiveness lasts only as long as someone supplies neutralizers. This is extremely costly and not very practical.

Wetland technologies are effective in treating the symptoms of pyrite oxidation when low levels of acidity are involved. However, "constructed wetlands"[42,56,78] as an AMD amelioration technology has limitations when the availability of H_2O is highly variable and high levels of acidity are involved. Also, many question the long-term effectiveness of such systems in the absence of any management. More importantly, however, "constructed wetlands" treat the symptoms of pyrite oxidation and not the problem itself, which is pyrite oxidation.

Novel microencapsulation (coating) technologies to prevent pyrite oxidation and acid production in pyritic wastes are currently under development in our laboratory. The first coating technology involves leaching coal waste with a solution composed of low but critical concentrations of H_2O_2, KH_2PO_4, and a pH buffer. During the leaching process, H_2O_2 oxidizes pyrite and produces Fe^{3+} so that iron phosphate precipitates as a coating on pyrite surfaces. The second coating technology involves leaching pyritic waste with a solution composed of low but critical concentrations of H_2O_2 and a pH buffer. During the leaching process, H_2O_2 oxidizes pyrite and produces an iron oxide coating on the surface of pyrite.

Successful application of these coating technologies in the field could mean a long-term solution to certain types of AMD problems.

ACKNOWLEDGMENTS

The work for this review (no. 94-3-57) was funded by the U.S. Geological Survey and the Kentucky Agricultural Experimental Station and is published with the approval of the director.

DISCLAIMER

The views and conclusions contained in this document are those of the authors and should not be interpreted as necessarily representing the official policies or recommendations of the Interior Department's U.S. Geological Survey (USGS) or of the U.S. Government.

REFERENCES

1. Ainsworth, C. C. and Blanchar,.R. W., Sulfate production rates in pyritic Pennsylvanian-aged shales, *J. Environ. Qual.,* 13, 93, 1984.
2. Arora, H. S., Dixon, J. B., and Hossner, L. R., Pyrite morphology in lignitic coal and associated strata of east Texas, *Soil Sci.,* 125, 151, 1978.
3. Asghar, M. and Kaehiron, Y., The fate of applied iron and manganese in an oxisol and an ultisol from Hawaii, *Soil Sci.,* 131, 53, 1981.
4. Aspiras, R. B., Keeney, D. R., and Chesters. G., Determination of reduced inorganic sulfur forms as sulphide by zinc-hydrochloric acid distillation, *Anal. Lett.,* 5, 425, 1972.
5. Baes, A. U. and Bloom. P. R., Diffuse reflectance and transmission fourier transform infrared, *Soil Sci. Am. J.,* 53, 695, 1989.
6. Bailey, L. K. and Peters. E., Decomposition of pyrite in acids by pressure leaching and anodization: The case for electrochemical mechanism, *Can. Met. Quart.,* 15, 333, 1976.
7. Baker, B. K., The Evaluation of Unique Acid Mine Drainage Abatement Techniques, M.S. thesis, West Virginia University, Morgantown, 1983.
8. Barnhisel, R. I. and Massey, H. F.,Chemical, mineralogical and physical properties of eastern Kentucky acid-forming coal spoil materials, *Soil Sci.,* 108, 367, 1969.
9. Barriga, F. J.A.S. and Fyfe, W. S., Giant pyritic base-metal deposits: the example of feitais (Aljustrel, Portugal). *Chem. Geol.,* 69, 331, 1988.
10. Bell, A. B., Prevention of acid generation in base metal tailings and waste rock. Proceedings of Acid Mine Drainage. Seminar and Workshop, March 23 to 26. Halifax, Nova Scotia, 1987.
11. Bennett, J. C. and Tributsch, H., Bacteria leaching patterns on pyrite crystal surface, *J. Bacteriol.,* 134, 310, 1978.
12. Berner, R. A.,Sedimentary pyrite oxidation. *Am., J. Sci.,* 268, 1. 1970.

13. Berner, R. A., Sedimentary pyrite formation: an update, *Geochim. Cosmochim. Acta,* 48, 605, 1984.
14. Blessing, N. V., Lackey, J. A., and Spry, A. H., *Minerals and Environment,* Jones, M. J., Ed., Institution of Mining, London, 1975, 341.
15. Brierley, C. L., Microbiological mining, *Sci. Am.,* 247, 42, 1982.
16. Brodie, G. A., Britt, C. R., Tomaszewski, T. M., and Taylor, H. M., Use of the passive anoxic limestone drains to enhance performance of acid drainage treatment wetlands, in Proceedings Reclamation 2000: Technologies for Success, Oaks, W. and Bowden, J., Eds., Durango, CO, 1991, 211.
17. Bronswijk, J. J. B. and Groenenberg, J. E., SMASS: a simulation model for acid sulfate soils. I. Basic principles. in Selected Pap. Saigon Symp. Acid Sulfate Soils, Ho Chi Minh City, Vietnam, March 2 to 6, 1992, ILRI Publ. 52, Dent, D. and van Mensvoort, M. E. F., Eds., Institute for Land Reclamation and Improvement, Wageningen, the Netherlands, 1993.
18. Bronswijk, J. J. B., Nugroho, K., Aribawa, I. B., Groenenberg, J. E., and Ritsema, C. J., Modeling of oxygen transport and pyrite oxidation in acid sulfate soils, *J. Environ. Qual.,* 22, 544, 1993.
19. Brown, A. D. and Jurinak, J. J., Mechanism of pyrite oxidation in aqueous mixtures, *J. Environ. Qual.,*18, 545, 1989.
20. Brown, A. D. and Jurinak, J. J., Mechanisms of nonmicrobial pyritic sulfur oxidation under alkaline conditions, *Arid Soil Res.,* 3, 65, 1989.
21. Carpenter, P. L., *Microbiology.,* W. B. Saunders Company, Philadelphia, PA, 1977, 218.
22. Carranza, F, Ph.D thesis, University of Seville, Seville, Spain,1983.
23. Caruccio, F. T., Estimating the acid potential of coal mine refuse,in *The Ecology of Resource Degradation and Renewal,* Chadwick, M. J. and Goodman, G. T., Eds., Blackwell Scientific, London, 1975.
24. Caruccio, F. T. and Geidel, G., Geochemical factors affecting coal mine drainage quality, in *Reclamation of Drastically Disturbed Lands,* Schaller, F. W. and Sutgton, P., Eds., Am. Soc. of Agron. Madison, WI, 1978, 129.
25. Caruccio, F. T. and Geidel, G., The assessment of a stratum's capacity to produce acidic drainage, in Proceedings of National Symposium on Surface Mine Hydrology, Sedimentology and Reclamation, University of Kentucky, Lexington KY, 1980, 437.
26. Caruccio, F. T. and Geidel, G., Estimating the minimum acid load that can be expected from a coal strip mine, in Proceedings of National Symposium on Surface Mine Hydrology, Sedimentology and Reclamation, University of Kentucky, Lexington, KY, 1981, 117.
27. Caruccio, F. T., Ferm, J. C., Horne, J., Geidel, G., and Baganz, B., Paleoenvironment of coal and its relation to drainage quality, EPA-600/7-77-067, Environmental Protection Agency, 1977.
28. Caruccio, F. T. and Geidel, G., The effect of plastic liner on acid loads/DLM site, W.V., in Proceedings, Fourth West Virginia Surface Mine Drainage Task Force Symposium, Clarksburg, WV, 1983.
29. Caruccio, F. T. and Geidel, G., The prediction of acid mine drainage from coal strip mines, Proc. Reclam. Aband. Acid Spoils, Missouri Department of Natural Resources Land Reclamation Commission, 1985.
30. Caruccio, F. T., Geidel, G., and Williams, R., Induced alkaline recharge trenches, an innovative method to bate acid mine drainage, in Proceedings of Sixth West Virginia Surface Mine Drainage Task Force Symposium, Morgantown, WV, 1985.
31. Chang, Y. C. and Myerson, A. S., Growth model of the continuous bacteria leaching of iron pyrite by *Thiobacillus ferrooxidans., Biotechnol. Bioeng.,* 24, 889, 1982.
32. Cormely, L. S., Duncan, D. W., Branion, R. M. R., and Pinder, K. L., 1975. Continuous culture of *Thiobacillus ferrooxidans., Biotechnol. Bioeng.,* 27, 1173, 1975.

33. de Donato, P. , Mustin, C., Berthelin, J., and Marion, P., An infrared investigation of pellicular phases observed on pyrite by scanning electron microscopy, during its bacteria oxidation, *C. R. Acad. Sci. Paris,* . 321, (II), 241, 1991.
34. Donato, P. de, Mustin, C., Benoit, R., and Erre, R., Spatial distribution of iron and sulphur species on the surface of pyrite, *Appl. Surf. Sci.,* 68, 81, 1993.
35. Dugan, P. R., Bacteria ecology of strip mine areas and its relationship to production of acidic mine drainage, *Ohio J. Sci.,* 75, 266, 1975.
36. Dugan, P. R., Prevention of formation of acid drainage from high-sulfur coal refuse by inhibition of iron- and sulfur-oxidizing microorganisms. II. Inhibition in "run of mine" refuse under simulated field conditions, *Biotechnol. Bioeng.,* 29, 49, 1987.
37. Dugan, P. R. and Apel, W. A., Bacteria and acidic drainage from coal refuse: inhibition by sodium lauryl sulfate and sodium benzoate, *Appl. Environ. Microbiol.,* 46, 279, 1983.
38. Eger, P., The use of sulfate reduction to remove metals from acid mine drainage, in Achieving Land Use Potential Through Reclamation, Proceedings of 9th National Meeting of the American Society for Surface Mining and Reclamation, Duluth, MN, June 14 to 18, 1992. 563.
39. Ehrlich, H. L., Bacterial oxidation of arsenopyrite and enargite, *Econ. Geol.,* 59, 1306, 1964.
40. Ehrlich, H. L., Bacterial action on orpiment, *Econ. Geol.,* 58, 991, 1963.
41. Erickson, P. M. and Ladwig, K. J., Control of Acid Formation by Inhibition of Bacteria and by Coating Pyritic Surfaces, Final Report to the West Virginia Department of Energy, Division of Reclamation, Charleston, WV, 1985.
42. Erickson, P. M., Girts, M. A., and Kleinmann, R. L. P., Use of constructed wetlands to treat coal mine drainage, in Proc. National Western Mining Conference, Denver, CO, February, 11 to 13, 1987.
43. Espejo, R. T. and Romero, P., Growth of *Thiobacillus ferroxidans* on elemental sulfur, *Appl. Environ. Microbiol.,* 53, 1907, 1987.
44. Evangelou, V. P., Pyrite/surface reactions, and their potential mechanistic influence on nonmicrobial pyrite oxidation, *J. Environ. Qual.,* submitted, 1994).
45. Evangelou, V. P., Remediation of Acid Drainage Through Surface Coating of Iron Sulfides, U. S. Geological Survey, Water Resources Research Act Grant Program (7846), 1994.
46. Evangelou, V. P. and Wang, J., Differences between infrared spectra of atrazine obtained under transmittance and diffuse reflectance modes, *Spectrochim. Acta,* 49A, 291, 1993.
47. Evangelou, V.P., Pyritic coal spoils: their chemistry and water interactions, in *Leaching and Diffusion.,* Augustithis, S. S., Ed., International Committee for the Studies of Bauxites, Alumina, and Aluminum, Theophrastis Publications, Athens, Greece, 1985, 175.
48. Evangelou, V.P. and Wagner, G. J., Effects of ion activity and sugar polyalcohol osmotica on ion uptake, *J. Exp. Botany,* 38, 1637, 1987.
49. Evangelou, V. P. and Huang, X., Infrared spectroscopic evidence of an iron(II)-carbonate complex on the surface of pyrite, *Spectrochim. Acta,* 50A, 1333, 1994.
50. Evangelou, V.P., Barfield, B. J., and Barnhisel, R. I., Modeling release of chemical constituents in surface mine runoff and in coal mine sedimentation ponds, *Trans. Am. Soc Agric Eng.,* 30, 82, 1987.
51. Evangelou, V.P., Sainju, U. M., and Huang, X., Evaluation and quantification of armoring mechanisms of calcite, dolomite and rock phosphate by manganese, in *Land Reclamation: Advances in Research and Technology,* Younos, T., Diplas, P., and Mostaghimi, S., Eds., American Society of Agricultural Engineers, Nashville, TN, 1992, 304.
52. Flynn, J.P., Treatment of Earth Surface and Subsurface for Prevention of Acidic Drainage from the Soil. US Patent 3,443,882, 1969.
53. Foreman, J. W., Evaluation of mine sealing in Butler County, Pennsylvania, in 4th Symp. Coal Mine Drainage Res., Louisville, KY, 1972, 83.
54. Fornasiero, D., Eijt, V., and Ralston, J., An electrokinetic study of pyrite oxidation, *Colloids Surf.,* 62, 63, 1992.

55. Giblin, A. E., Pyrite formation in marshes during early diagnoses, *Biotecnol. Bioeng.*, 9, 471, 1988.
56. Girts, M. A. and Kleinmann, R. L. P., Constructed wetlands for treatment of acid mine drainage: a preliminary review, in National Symposium on Mining, Hydrology, Sedimentology, and Reclamation, University of Kentucky, Lexington, 1986.
57. Goldhaber M. B., Experimental study of metastable sulfur oxyanion formation during pyrite oxidation at pH 6-9 and 30°C, *Am. J. Sci.*, 283, 913, 1983.
58. Goldhaber, M. B. and I. Kalan, I. R., The sulfur cycle, in The Sea, Vol. 5, *Marine Chemistry*, Goldberg, E. D., Ed., Wiley-Interscience, New York, 1974, 527.
59. Gormely, L. S., Duncan, D. W., Branion, R. M. R., and Pinder, K. L., Continuous culture of *Thiobacillus ferrooxidans* on a zinc sulfide concentrate, *Biotechnol. Bioeng.*, 17, 31, 1975.
60. Goto, K., Tamura, H., and Nagayama, M., The mechanism of oxygenation of ferrous ion in natural solution, *Inorg. Chem.*, 9, 963, 1970.
61. Grady, W. C., Microscopic varieties of pyrite in West Virginia coals, *Trans. Soc. Min. Eng. AIME*, 262, 268, 1977.
62. Greer, R. T., Coal microstructure and the significance of pyrite inclusions, *Scanning Electron Microsc.*, 10, 79, 1977.
63. Hamilton, I. C. and Woods, R., An investigation of surface oxidation of pyrite and pyrrhotite by linear potential sweep voltammetry, *J. Electroanal Chem.*, 118, 327, 1981.
64. Hammack R. W. and Watzlaf, G. R., The effect of oxygen on pyrite oxidation, in Proceedings of the Mining and Reclamation Conference, Charleston, WV, April 23 to 26, 1990, 257.
65. Hammack, R. W. and Edenborn, H. M., The removal of nickel from mine waters using bacteria sulfate reduction, in Proceeding of the 1991 National Meeting of the American Society of Surface Mining and Reclamation, Oaks, W. and Bowden, J., Eds., Princeton, WV, Vol. 1, 97.
66. Harrison, A. P., The acidophilic thiobacilli and other acidophilic bacteria that share their habitat, *Annu. Rev. Microbiol.*, 38, 265, 1984.
67. Harter, R. D. and Ahlrichs, J. L., Determination of clay surface acidity by infrared spectroscopy, *Soil Sci. Soc. Am. Proc.*, 31, 30, 1967.
68. Hider, R. C., Siderophore mediated absorption of iron, *Struct. Bond.*, 58, 26, 1984.
69. Hoffmann, M. R. , Faust, B. C., Panda, F. A., Koo, H. H., and Tsuchiya, H. M., Kinetics of the removal of iron pyrite from coal by microbial catalysis, *Appl. Environ. Microbiol.*, 42, 259, 1981.
70. Hood, T. A., The Kinetics of Pyrite Oxidation in Marine Systems, Ph.D. thesis, University of Miami. Coral Gables, FL, 1991.
71. Howarth, R. W. and Teal, J. M., Sulfur reduction in New England salt marsh, *Limnol. Oceanogr.*, 24, 999, 1979.
72. Huang, X. and Evangelou, V. P., Abatement of Acid Mine Drainage by Encapsulation of Acid Producing Geologic Materials, U. S. Department of the Interior, Bureau of Mines, 1992.
73. Huang, X. and Evangelou, V. P., Kinetics of pyrite oxidation and surface chemistry influences, in *The Environmental Geochemistry of Sulfide Oxidation*, Alpers, C. N. and Blowes, D. W., Eds., American Chemical Society, Washington, D.C., 1994, 562.
74. Ivanov, V.I., Effect of some factors on iron oxidation by cultures of *Thiobacillus ferrooxidans*, *Microbiology*, 31, 645, 1962.
75. Jackson, M. L., Stewart, B. R., and Daniels, W. L., Influence of flyash, topsoil, lime and rock-P on acid mine drainage from coal refuse, in Proceedings of 1993 National Meeting of the American Society for Surface Mining and Reclamation, Spokane, WA, May 16 to 19, 1993, 266.
76. Jaynes, D.B., Rogowski, A.S., and Pionke, H. B., Acid mine drainage from reclaimed coal strip mines. I. Model description, *Water Res. Res.*, 20, 233, 1984.
77. Kleinmann, R. L. P., Acid mine drainage: U.S. Bureau of mine researches and develops control methods for both coal and metal mines. *E&MJ.*, July 1989, 16I.

78. Kleinmann, R. L. P., Treatment of acid mine water by wetlands, in Control of Acid Mine Drainage, IC 9027, U.S. Department of Agriculture, Bureau of Mines, Pittsburgh, PA, 1985.
79. Kleinmann, R. L. P., The U.S. Bureau of Mines acid mine drainage research program, in Proceedings Second West Virginia Surface Mine Drainage Task Force Symposium, Clarksburg, WV, 1981.
80. Kleinmann, R. L. P. and Crerar, D. A., *Thiobacillus ferrooxidans* and the formation of acidity in simulated coal mine environments, *Geomicrobiol. J.*, 1, 373, 1979.
81. Kleinmann, R.L.P., Bactericidal control of acid problems in surface mines and coal refuse, in Proceedings of National Symposium of Surface Mining Hydrology, Sedimentology and Reclamation, University of Kentucky, Lexington, 1980, 31.
82. Konishi, Y., Asai, S., and Sakai, H. K., Bacteria dissolution of pyrite by *Thiobacillus ferrooxidans.*, *Bioprocess Eng.*, 5, 231, 1990.
83. Ladwig, K. J., Erickson, P. M., and Kleinmann, R. L. P., Alkaline injection: an overview of recent work, in Control of Acid Mine Drainage, IC 9027, U.S. Department of Agriculture, Bureau of Mines, Pittsburgh, PA, 1985, 35.
84. Lasaga, A. C., Rate laws of chemical reactions, *Rev. Mineral.*, 8, 1, 1981.
85. Lekhakul, S., The Effect of Lime on the Chemical Composition of Surface Mined Coal Spoils, and the Leachate from Spoil, Ph.D. thesis, Agronomy Department, University. of Kentucky, Lexington, 1981, 134.
86. LeRoux, N. W., Dacey, P. W., and Temple, K. L., The microbial role in pyrite oxidation at alkaline pH in coal mine spoil, in *Biogeochemistry of Ancient and Modern Environments*, Truidnger, P. A., Walter, M. R., and Ralph, B. J., Eds., Springer-Verlag, Berlin, 1980, 515.
87. Lindsay, W. L., *Chemical Equilibria in Soil*, John Wiley & Sons, New York, 1979.
88. Lizama, H. M. and Suzuki, I., Rate equation and kinetic parameters of the reactions involved in pyrite oxidation by *Thiobacillus ferrooxidans*, *Appl. Environ. Microbiol.*, 55, 2918, 1989.
89. Loomis, E.C. and Hood, W. C., The effects of anaerobically digested sludge on the oxidation of pyrite and the formation of acid mine drainage, in Proceedings of National Symposium of Surface Mining Hydrology, Sedimentology and Reclamation, University of Kentucky, College of Engineering, Lexington, 1984, 1.
90. Lorenz, W. C. and Tarpley, E. C., Oxidation of Coal Mine Pyrites, RI 6247, U.S. Bureau of Mines, 1963.
91. Lowson, R. T., Aqueous oxidation of pyrite by molecular oxygen, *Chem. Rev.*, 82, 461, 1982.
92. Lundgren, D. G. and Silver, M., Ore leaching by bacteria, *Annu. Rev. Microbiol.*, 34, 263, 1980.
93. Lundgren, D. G., Vestal, J. R., and Tabita, F. R., *Water Polution Microbiology*, Wiley-Interscience, New York, 1972.
94. Luther, G. W., III, Pyrite and oxidized iron mineral phases from pyrite oxidation in salt marsh and estuarine sediments, *Geochim. Cosmochim. Acta*, 46, 2665, 1982.
95. Luther, G. W., III, The frontier-molecular-orbital theory approach in geotechnical processes, in *Aquatic Chemical Kinetics*, Stumm, W., Ed., John Wiley & Sons, New York, 1990, 173.
96. Luther, G. W., III, Pyrite oxidation and reduction: molecular orbital theory consideration, *Geochem. Cosmochem. Acta*, 51, 3193, 1987.
97. Luther, G. W., III, Kostka, J. E., Church, T. M., Sulzberger, B., and Stumm, W., Seasonal iron cycling in the salt-marsh sedimentary environment: the importance of ligand complexes with Fe(II) and Fe(III) in the dissolution of Fe(III) minerals and pyrite, respectively, *Marine Chem.*, 40, 81, 1992.
98. Mckibben M. A. and Barnes, H. L., Oxidation of pyrite in low temperature acidic solutions: rate laws and surface textures, *Geochim. Cosmochim. Acta*, 50, 1509, 1986.
99. Mehta, A. P. and Murr, L. E., Fundamental studies of the contribution of galvanic interaction to acid-bacterial leaching of mixed metal sulfides, *Hydrometallurgy*, 9, 235, 1983.

100. Mehta, A. P. and Murr, L. E., Fundamental studies of the contribution of galvanic interaction to acid-bacterial leaching of mixed metal sulfides, *Hydrometallurgy*, 9, 235, 1983.
101. Millero, F. J., The effect of ionic interactions on the oxidation of metals in natural waters, *Geochim. Cosmochim. Acta*, 49, 547, 1985.
102. Millero, F. J. and Izaguirre, M., Effect of ionic strength and ionic interactions on the oxidation of Fe^{2+}, *J. Solute Chem.*,18, 585, 1989.
103. Mortland, M. M., Protonation of compounds on clay mineral surfaces, in 9th Int. Congr. Soil Sci., Vol. 1, 1968, 691.
104. Mortland, M. M. and Raman, K. V., Surface acidity of smectites in relation to hydration, exchangeable cation and structure, *Clays Clay Miner.*, 16, 393, 1968.
105. Moses, C. O. and Herman, J. S., Pyrite oxidation at circumneutral pH, *Geochim. Cosmochim. Acta*, 55, 471, 1991.
106. Moses, C. O., Nordstrom, D. K., Herman, J. S., and Mills, A. L., Aqueous pyrite oxidation by dissolved oxygen and by ferric iron, *Geochim. Cosmochim. Acta*, 51, 1561, 1987.
107. Murthy, A. R. V. and Sharada, K., Determination of sulfide sulfur in minerals, *Analyst*, 85, 299, 1960.
108. Mustin, C., Berthelin, J., Marion, P., and de Donato, P., Corrosion and electrochemical oxidation of a pyrite by *Thiobacillus ferrooxidans*, *Appl. Environ. Microbiol.*, 58, 1175, 1992.
109. Nairn, R. W., Hedin, R. S., and Watzlaf, G. R., A preliminary review of the use of anoxic limestone drains in the passive treatment of acid mine drainage, in Proceedings of the 12th Annual West Virginia Surface Mine Drainage Task Force Symposium, Morgantown, WV, 1991, 23.
110. Nairn, R. W., Hedin, R. S., and Watzlaf, G. R., Generation of alkalinity in an anoxic limestone drain, in Proceedings of the 9th Annual Meeting of the American Society for Surface Mining and Reclamation, Duluth, MN, June 14 to 18, 1992.
111. Nicholson, R. V., Gillham, R. W., and Reardon, E. J., Pyrite oxidation in carbonate-buffered solution. I. Experimental kinetics, *Geochim. Cosmochim. Acta*, 52, 1077, 1988.
112. Nicholson, R. V., Gillham, R. W., and Reardon, E. J., Pyrite oxidation in carbonate-buffered solution. II. Rate control by oxide coatings, *Geochim. Cosmochim. Acta* , 54, 395, 1990.
113. Nordstrom, D. K., Aqueous pyrite oxidation and the consequent formation of secondary iron minerals, in Acid Sulfate Weathering: Pedogeochemistry and Relationship to Manipulation of Soil Minerals. Hossner, L. R., Kittrick, J. A., and Fanning, D. F., Eds., Soil Science Society of America Press, Madison, WI, 1982, 46.
114. O'Shay, T., Hossner, L. R., and Dixon, J. B., A modified hydrogen peroxide oxidation method for determination of potential acidity in pyritic overburden, *J. Environ. Qual.*, 19, 778, 1990.
115. Ohio State University Research Foundation, Acid Mine Drainage Formation and Abatement, Water Pollut. Control Res. Ser. DAST-42-14210 FPR-04/71, U.S. Environmental Protection Agency, Washington, D.C., 1971.
116. Palencia, I, R., Wan, W., and Miller, J. D., The electrochemical behavior of a semiconducting natural pyrite in the presence of bacteria, *Metall. Trans. B*, 22, 765, 1991.
117. Pesic, B. D., Oliver, J., and Wichlacz, P., An electrochemical method of measuring rate of ferrous to ferric iron with oxygen in the presence of *Thiobacillus ferrooxidans.*, *Biotech. Bioengr.*, 33, 428, 1989.
118. Pionke, H. B., Rogowski, A. S., and Deangelis, R. J., Controlling the rate of acid loss from strip mine spoil, *J. Environ. Qual.*, 9, 694, 1980.
119. Rastogi, V., Krecic, R., and Sobek, A., ProMac systems for reclamation and control of acid production in toxic mine waste, in Proceedings Seventh West Virginia Surface Mine Drainage Task Force Symposium, Morgantown, WV, 1986.
120. Rees, W. J. and Sidrak, G. H., Plant nutrition on flyash, *Plant Soil*, 8, 141, 1956.

121. Renton, J. J., Stiller, A. H., and Rymer, T., The use of phosphate materials as ameliorates for acid mine drainage, in *Mine Drainage and Surface Mine Reclamation,* Vol. 1, *Mine Water and Mine Waste,* 1991, 67.
122. Richard, D. T., Kinetics and mechanism of pyrite formation at low temperatures, *Am. J. Sci.,* 275, 636, 1975.
123. Ritcey, G. M., Deep water disposal of pyritic tailings, in Proceedings of the Second International Conference on the Batement of Acidic Drainage, Montreal, Quebec, September 16 to 18, 1991, 421.
124. Ritsema, C. J. and Groennenberg, J. E., Pyrite oxidation, carbonate weathering, and gypsum formation in a drained potential acid sulfate soil, *Soil Sci. Am. J.,* 57, 968, 1993.
125. Scharer, J. M., Garga, V., Smith, R., and Halbert, B. E., Use of steady state models for assessing acid generation in pyritic mine tailings, in The Second National Conference on the Abatement of Acidic Drainage, Vol. 2, Montreal, Canada, September 16 to 18, 1991, 211.
126. Shellhorn, M. and Rastogi, V., Practical control of acid mine drainage using bactericides. In: Proceedings, Sixth West Virginia Surface Mine Drainage Task Force Symposium. Morgantown, WV, 1985.
127. Silver, M., The mechanism of iron-oxidizing thiobacilli, in *Metallurgical Application of Bacteria Leaching and Related Microbiological Phenomena,* Murr, L. E., Torma, A. E., and Brierley, J. A., Eds., Academic Press, New York, 1978.
128. Silverman, M. P, Mechanism of bacterial pyrite oxidation, *J. Bacteriol.,* 99, 1046, 1967.
129. Singer, P.C. and Stumm, W., Acid mine drainage: rate-determining step, *Science,* 167, 1121, 1970.
130. Skousen, J. G., Sencindiver, J. C., and Smith, R. M., Procedures for Mining and Reclamation in Areas with Acid-Producing Materials, Surface Mine Drainage Task Force and West Virginia University Energy Research Center, 1987, 43.
131. Smith, E. E. and Shumate, K. S., Sulfide to Sulfate Reaction Mechanism, Water Pollution Control Research Series, U.S. Department of the Interior, 1970.
132. Smith, R. M. and Sobek, A. A., Physical and chemical properties of overburdens, spoils, wastes, and new soils, in *Reclamation of Drastically Disturbed Lands,* Schaller, F. W. and Sutton, P., Eds., American Society of Agronomy, Madison, WI, 1978, 149.
133. Sobek, A. A., Shuller, W. A., Freeman, J. R., and Smith, R. M., Field and Laboratory Methods Applicable to Overburdens and Minesoils, EPA-600/2-78-054. U.S. Environmental Protection Agency, Cincinnati, OH, 1978.
134. Sorenson, D. L., Kneib, W. A., and Porcella, D. B., Determination of sulfide in pyritic soils and minerals with a sulfide ion electrode, *Anal. Chem.,* 51, 1870, 1979.
135. Sposito, G., *The Surface Chemistry of Soils,* Oxford University Press, New York, 1984.
136. Sposito, G. and Mattigod, S. V., GEOCHEM: A Computer Program for the Calculation of Chemical Equilibria in Soil Solutions and Other Natural Water Systems, Kearney Foundation of Soil Science, University of California, Riverside, 1979.
137. Spotts, E. and Dollhopf, D. J., Evaluation of phosphate materials for control of acid production in pyritic mine overburden, *J. Environ. Qual.,* 21, 627, 1992
138. Staub, M. W. and Cohen, R. R. H., A passive mine drainage treatment system as a bioreactor: treatment efficiency, pH increase, and sulfate reduction in two parallel reactors, in *Achieving Land Use Potential Through the Reclamation,* Proceedings of the 9th National Meeting of the American Society of Surface Mining and Reclamation, Duluth, MN, June 14-18, 1992, 550.
139. Stiller, A. H., Renton, J. J., and Rymer, T. E., The use of phosphates for ameliorization, in Proceedings Seventh West Virginia Surface Mine Drainage Task Force Symposium, Morgantown, WV, 1986.
140. Stiller, A. H., Renton, J. J., Rymer, T. E., and McConaghy, B. G., The effect of limestone treatment on the production of acid from toxic mine waste in barrel scale weathering experi-

ments, in Proceedings Fifth West Virginia Surface Mine Drain Task Force Symposium, Morgantown, WV, 1984, 90.

141. Stumm. W. and Morgan, J. J., *Aquatic Chemistry,* John Wiley & Sons, New York, 1970.
142. Stumm. W. and Morgan, J. J., *Aquatic Chemistry,* John Wiley & Sons, New York, 1970, 583.
143. Sturey, C. S., Freeman, J. R., Keeney, T. A., and Sturm, J. W., Overburden analysis by acid-base accounting and simulated weathering studies as a means of determining the probable hydrological consquences of mining and reclamation, in Proceedings Symposium on Surface Mining, Hydrology, Sedimentology, and Reclamation, University of Kentucky, Lexington, 1982, 163.
144. Suzuki, I., Lizama, H. M., and Tackaberry, P. D., Competitive inhibition of ferrous iron oxidation by *Thiobacillus ferrooxidans* by increasing concentrations of cells, *Appl. Environ. Microbiol.,* 55, 1117, 1989.
145. Taylor, B. E., Wheeler,M. C., and Nordstrom, D. K., Stable isotope geochemistry of acid mine drainage: experimental oxidation of pyrite, *Geochim. Cosmochim. Acta,* 48, 2669, 1984.
146. Taylor, B. E., Wheeler, M. C., and Nordstrom, D. K., Oxygen and sulfur compositions of sulfate in acid mine drainage: evidence for oxidation mechanism, *Nature (London),* 308, 538, 1984.
147. Torma, A. E., Osoka, A. S., and Valayapetre, M., Electrochemical method in recovery of metal from sulfide minerals, *Res. Assoc. Miner. Sarda.,* 84, 5, 1979.
148. Torma, A. E., Leaching of metals, in *Biotechnology,* Vol. 6B, Rehm, H. J. and Reed, G., Eds., VCH Verlagsgesellschaft, Weinheim, Germany, 1988, 367.
149. Turner, D. and McCoy. D., Anoxic alkaline drain treatment system, a low cost acid mine drainage treatment alternative, in Proceedings of the 1990 National Symposium on Mining, Graves, D. H. and De Vore, R. W., Eds., Lexington, KY, 1990, 73.
150. U.S. Environmental Protection Agency, Design Manual: Neutralization of Acid Mine Drainage, Office of Research and Development, Industrial Environmental Research Laboratory, 1983.
151. Wakao, N., Mishina, M., Sakurai, Y., and Shiota, H., Bacteria pyrite oxidation. I.The effect of the pure and mixed cultures of *Thiobacillus ferrooxidans* and *Thiobacillus thiooxidans* on release of iron, *J. Gen. Appl. Microbiol.,* 28, 331, 1982.
152. Wakao, N., Mishina, M., Sakurai, Y., and Shiota, H., Bacteria pyrite oxidation. II. The effect of varous organic substances on release of iron from pyrite by *Thiobacillus ferrooxidans, J. Gen. Appl. Microbiol.,* 29, 177, 1983.
153. Wakao, N., Mishina, M., Sakurai, Y., and Shiota, H., Bacteria pyrite oxidation. III. Adsorption of *Thiobacillus ferrooxidans* on solid surfaces and its effect on iron release from pyrite, *J. Gen. Appl. Microbiol.,* 30, 63, 1984.
154. Watzlaf, G. R., Pyrite oxidation in saturated and unsaturated coal waste. in Proceedings of 9th National Meeting of the American Society for Surface Mining and Reclamation, Duluth, MN, June 14 to 18, 1992, 191.
155. Watzlaf, G. R. and Hedin, R. S., A method for predicting alkalinity generated by anoxic limestone drains, in Proceedings of the 1993 West Virginia Surface Mine Drainage Task Force Symposium, Morgantown, WV, April 27 to 28, 1993.
156. Wentzler, T. H. and Aphan, F. F., Kinetics of limestone dissolution by acid waste waters, in *Environmental Control,* Rampacek, C., Ed., San Francisco, CA, 1972, 513.
157. Wiersma, C. L. and Rimstidt, J. D., Rate of reaction of pyrite and marcasite with ferric iron at pH 2, *Geochim. Cosmochim. Acta,* 48, 85, 1984.
158. Wildeman, T. R., Drainage from coal mine: chemistry and environmental problems, in *Geology in Coal Reosurce Utilization.,* Peters, D. C., Ed., Techbooks, Fairfax, VA, 1991, 499.
159. Zhang, Y. L., Blanchar, R. W., and Hammer, R. D., Composition and pyrite morphology of materials separated from coal, in Proceedings of 10th National Meeting of American Society of Surface Mining and Reclamation, Vol. 2, Spokane, WA, May 16 to 19, 1993, 284.
160. Zhang, Y. L., Chemistry of Fly Ash Scrubber Sludge Components in Plant-Soil-Water Systems, Ph.D. thesis, University of Missouri-Columbia, 1993.